Drug Design, Development and Therapy

Dovepress
Taylor & Francis Group

Open Access Full Text Article

REVIEW

Engineered Delivery Systems for Chinese Herbal Medicine in Peripheral Nerve Regeneration: Challenges, Advances, and Future Perspectives

Ruirui Zhang[1,2,*], Miao Gu[3,*], Rui Ma[2], Rong Li[1], Shijie Xu[1], Zhipeng Xu[4]

[1]Jiangsu Province Key Laboratory of Medical Science and Laboratory Medicine, Department of Laboratory Medicine, School of Medicine, Jiangsu University, Zhenjiang, Jiangsu, 212013, People's Republic of China; [2]Department of Anatomy, School of Medicine, Jiangsu University, Zhenjiang, 212013, People's Republic of China; [3]Hebei Key Laboratory of Nerve Injury and Repair, Chengde Medical University, Chengde, Hebei, People's Republic of China; [4]Department of Urology, Affiliated People's Hospital of Jiangsu University, The First People's Hospital of Zhenjiang, Zhenjiang, Jiangsu, 212002, People's Republic of China

*These authors contributed equally to this work

Correspondence: Ruirui Zhang; Zhipeng Xu, Email zrr812124246@163.com; xuzhipeng880315@sina.com

Abstract: Peripheral neuropathy (PN), characterized by sensory, motor, and autonomic dysfunction, presents a significant therapeutic challenge owing to its diverse etiologies, dynamic spatiotemporal injury microenvironment, and impermeable blood-nerve barrier (BNB). The current treatment is mainly palliative and symptom-focused, and fails to solve the core pathological complexity, including the heterogeneity of nerve injury, the conflicting phases of inflammation, repair, and fibrosis, and the imbalance of the microenvironment in chronic conditions such as diabetes. Chinese herbal medicine (CHM) has multiple benefits including neuroprotective, anti-inflammatory, anti-oxidant, and microenvironmental regulation. However, its clinical translation is hindered by poor bioavailability, non-targeted biodistribution, BNB exclusion, and physicochemical mismatches in multicomponent formulations. Preclinical studies suggest that engineered delivery systems could emerge as a transformative solution to these limitations. Nanocarriers penetrate the BNB via diffusion or ligand-mediated targeting, offering spatiotemporal control through a stimulus-responsive design. Hydrogels align their degradation processes with nerve regeneration and correct the imbalanced microenvironments. Degradable membranes offer localized, sustained release, whereas functionalized nerve conduits address structural defects and improve functional recovery beyond autograft limitations. Despite promising preclinical efficacy, clinical translation faces significant hurdles, including long-term biocompatibility concerns, inconsistent scalability in manufacturing, dosage optimization balancing efficacy and cytotoxicity, dependence on external stimuli, and a lack of standardized regulatory frameworks. Overcoming these challenges requires interdisciplinary collaboration to advance intelligent multifunctional designs, scalable production, and rigorous validations. Based on compelling preclinical data, engineered CHM delivery systems are hypothesized to have enormous potential to transform PN management from palliative care to restorative treatment and establish a new framework in precision neurology.

Keywords: peripheral neuropathy, Chinese herbal medicine, CHM, engineered delivery systems

Introduction

Peripheral neuropathy (PN) encompasses a range of disorders characterized by sensory, motor, and autonomic dysfunctions, representing a substantial and growing global health challenge.[1] It is estimated that PN affects millions of people worldwide, with a prevalence rising sharply with age to afflict up to 20% of the population over the age of 60.[2–4] Diabetic peripheral neuropathy (DPN), one of the most common forms, exemplifies this burden, impacting approximately 50% of all diabetic patients over their lifetime.[5] These patients experience symptoms such as numbness, neuropathic pain, and impaired bodily functions.[6,7] With various etiologies including metabolic disorders, trauma, infections, and toxins, PN constitutes a significant therapeutic burden for which current therapies cannot cure.[8,9] The existing strategies mainly focus on symptomatic treatment. For DPN), glycemic control has shown inconsistent effectiveness, and first-line pain

Received: 28 August 2025
Accepted: 10 November 2025
Published: 18 November 2025

Graphical Abstract

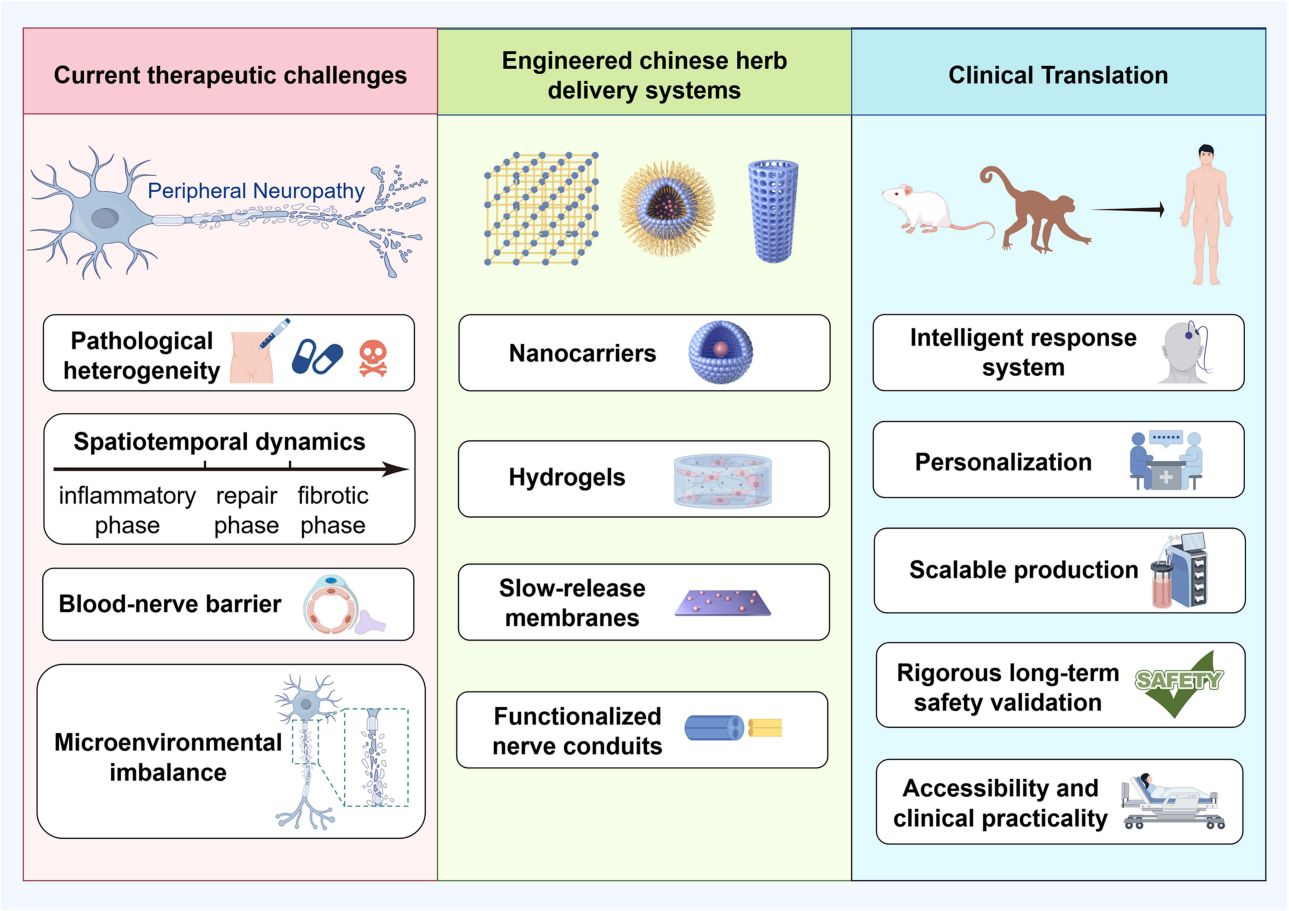

relievers such as duloxetine and pregabalin offer limited symptom relief, complicated by side effects and dosing issues.[10,11] The treatment of chemotherapy-induced peripheral neuropathy (CIPN) is similarly challenging, with a significant proportion of patients enduring symptoms even after discontinuing chemotherapy.[12] Current management strategies emphasize the importance of early detection and dose adjustment to minimize neurotoxicity, while maintaining anti-tumor efficacy.[13] Novel approaches, such as high-concentration capsaicin and intravenous lidocaine infusions, have shown potential in reducing neuropathic pain from CIPN, but further studies are necessary to ensure their long-term safety.[14,15] This therapeutic deficiency is due to core biological challenges: the pathological heterogeneity demanding etiology-specific interventions;[16] and the dynamic spatiotemporal evolution of nerve injury microenvironments through conflicting inflammatory, reparative, and fibrotic phases.[17–19] In addition, the systemic administration of drugs is a conventional approach for delivering therapeutic agents to injury sites. However, the effectiveness of this approach is substantially limited by the blood-nerve barrier (BNB), which is a highly selective protective shield that prevents most drugs from entering the injury site via the circulatory system.[20,21] In addition, severe structural damage (>3 cm nerve gaps) exceeds the endogenous regenerative capacity, whereas conventional reconstructive techniques have biological and mechanical limitations.[22,23]

Chinese herbal medicine (CHM), traditionally administered as decoctions or oral powders, has long been recognized for its therapeutic potential for a wide range of medical conditions.[24] It offers a promising multifactorial alternative through neuroprotective, anti-inflammatory, anti-oxidant, and microenvironment-modulating bioactivities.[25] Yet, these

conventional forms inherently suffer from substantial pharmacological drawbacks that severely limit their clinical translation, such as poor oral bioavailability of bioactive constituents,[26] non-targeted biodistribution resulting in insufficient nerve accumulation,[27] BNB impermeability to complex phytomolecules,[28] and physicochemical incompatibilities in multi-component formulations that undermine their ability to work synergistically.[29] Recent advancements in engineered delivery systems, particularly those utilizing nanotechnology, hydrogels, degradable membranes, and functionalized nerve conduits, offer promising solutions to these challenges.

Furthermore, this review provides a novel conceptual framework that systematically links the multifaceted therapeutic challenges of PN, such as pathological heterogeneity, spatiotemporal dynamics, BNB impermeability, microenvironment imbalance, and structural defects, with the design features of engineered delivery systems. We propose a structured decision classification to guide the selection of appropriate delivery platforms, such as nanocarriers, hydrogels, degradable membranes or functionalized nerve conduits, according to specific pathological phases and biological barriers. This framework is cross-referenced throughout the review to clarify when and why a particular system is advantageous, providing a strategic roadmap for the rational design and clinical translation of CHM-based therapies for PN.

This review comprehensively examined the burgeoning field of engineered CHM delivery systems for PN. As a narrative review, it aims to provide a broad, critical, and synthesized overview of the current state of the art, identify key challenges, and propose a novel conceptual framework for the field, rather than to systematically evaluate all available evidence. We first outline the complex therapeutic challenges that current strategies fail to adequately resolve, and critically analyze the inherent limitations of CHM that impede its clinical efficacy despite its therapeutic potential. The core focus is on innovative engineering solutions, where we dissect the design principles, mechanisms of action, preclinical efficacy, and persisting translational hurdles of key delivery platforms, including nanocarriers, hydrogels, degradable slow-release membranes, and functionalized nerve conduits. By integrating these advanced techniques and materials, our review not only presents a distinct viewpoint but also provides a clear strategy for addressing existing challenges in conventional CHM delivery. By synthesizing promising preclinical cases, this review aims to propose a conceptual framework that could establish a new standard for future research (Figure 1).

Therapeutic Challenges and Current Treatment Limitations in Peripheral Neuropathy

Pathological Heterogeneity Challenge

PN encompasses diverse etiologies such as mechanical trauma, metabolic dysfunction, inflammation, infection, malignancy, inherited disease, drugs, and toxins, each demanding a distinct therapeutic strategy.[16] However, current treatments have failed to address this heterogeneity. Similarly, drug treatments such as methylcobalamin injections cannot concurrently resolve different pathologies. However, they do not sufficiently accelerate axonal regeneration to prevent irreversible muscle atrophy.[30]

Spatiotemporal Dynamics Challenge

The injury microenvironment evolves through three phases with conflicting therapeutic requirements: an early inflammatory phase dominated by TNF-α/IL-1β rise sharply,[17] a repair phase dependent on Schwann cells (SCs) dedifferentiation and neurotrophic factors secretion,[18] and a late fibrotic Phase In which collagen deposition blocks regeneration.[19] Current therapies lack spatiotemporal adaptability. For example, early anti-inflammatory drugs may alter the inflammatory nerve microenvironment, inadvertently inhibiting SCs dedifferentiation, and weakening repair mechanisms.[31] Systemically administered neurotrophic factors have low bioavailability at lesion sites owing to rapid clearance and missing critical phase-specific windows.[28] However, single-type drug formulas cannot be adapted to these shifts.

Biological Barrier Challenge

BNB is a critical component of the peripheral nervous system and serves as a protective shield that maintains homeostasis of the neural environments.[32] However, its highly selective nature poses significant challenges for the delivery of large therapeutic molecules, which has garnered considerable attention in recent research. BNB is composed of highly

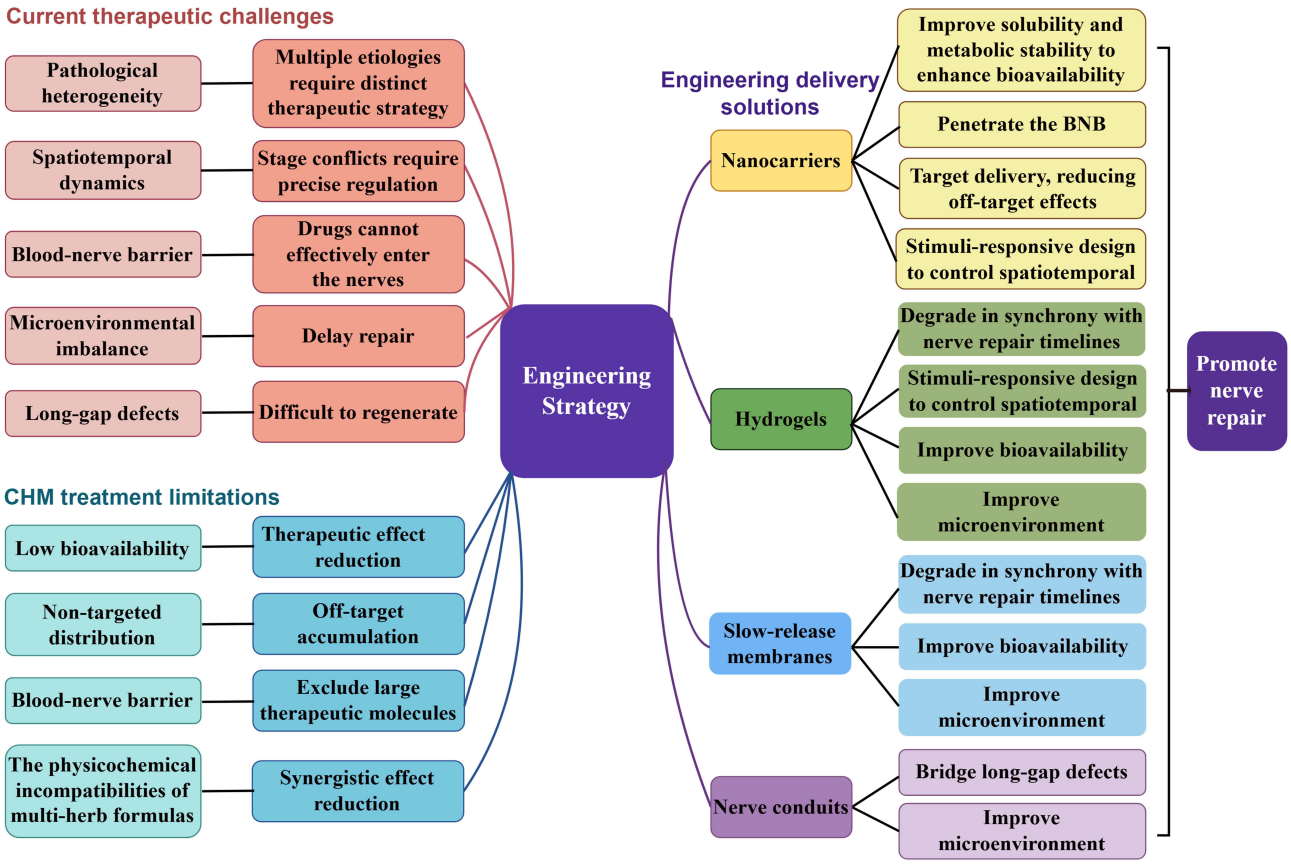

Figure 1 Engineered delivery systems overcoming multifaceted barriers in PN treatment. Current therapeutic challenges in nerve repair involve: pathological heterogeneity (requiring distinct strategies for multiple etiologies); spatiotemporal dynamics (demanding precise regulation due to stage conflicts); the blood-nerve barrier (BNB, hindering effective drug penetration into nerves); microenvironmental imbalance (delaying regenerative processes); and long-gap defects (impeding regeneration). Limitations of CHM therapy include: low bioavailability (compromising therapeutic efficacy); non-targeted distribution (causing off-target accumulation); BNB-mediated exclusion of large therapeutic molecules; and physicochemical incompatibilities of multi-herb formulas (reducing synergistic effects). Engineered delivery systems resolve these barriers through four synergistic strategies: (1) Nanocarriers enhance bioavailability, penetrate the BNB, enable targeted delivery, and allow stimuli-responsive spatiotemporal control; (2) Hydrogels degrade synchronously with nerve repair timelines, enable stimuli-responsive spatiotemporal regulation, enhance bioavailability, and modulate the local microenvironment; (3) Slow-release membranes also degrade in sync with nerve repair timelines, improve bioavailability, and optimize the microenvironment; (4) Nerve conduits bridge long-gap defects and ameliorate the microenvironment. Collectively, these engineering approaches overcome critical barriers to promote nerve repair. (By Figdraw).

specialized endothelial cells, perineurial cells, SCs, pericytes, basement membranes, and invested axons.[33] The more extensively studied blood-brain barrier (BBB) is characterized by its unique structural and functional properties, including specialized tight junctions and transport mechanisms that restrict the passage of substances.[34] This selectivity is crucial for protecting peripheral nerves but simultaneously complicates therapeutic interventions aimed at treating neuropathies and other nerve-related conditions. For example, it prevents the transmission of large molecules such as IgG antibodies, nerve growth factors, and albumin through the body.[33] This limits the effectiveness of the traditional treatments. For example, neurotrophic agents such as methylcobalamin have no significant effect on the treatment of painful diabetic neuropathy.[35] Oral analgesics such as gabapentin accumulate predominantly in the liver and kidneys,[36] causing systemic toxicity without overcoming BNB exclusion.

Microenvironmental Imbalance Challenge

Chronic conditions, such as diabetes, induce severe microenvironmental dysregulation, elevating M1/M2 macrophage ratios to delay repair.[37] SCs under hyperglycemic conditions show impaired production and secretion of neurotrophic factors, thereby hindering regeneration.[38] Although stem cells improve neurological function and alleviate clinical symptoms through secretion of neurotrophic factors and immune regulation, different stages of the disease may require different types, doses, and injection routes of stem cells, and long-term risks require more comprehensive observation.[39]

This dysregulation fundamentally undermines treatment efficacy. Even for specific symptoms of neuropathic pain in DPN, where pharmacological options exist, significant limitations persist, and Duloxetine and Pregabalin are the only drugs approved by the US Food and Drug Administration (FDA) for treating painful DPN. However, these drugs are only effective in approximately 40% of patients.[40] This exemplifies the broader challenge of achieving adequate symptom control, let alone modifying the underlying disease process, across neuropathies characterized by microenvironmental derangement.

Structural Repair Challenge

Long-gap defects (>3 cm) make it impossible to repair them with internal regeneration ability.[41] Autologous remains the gold standard for gaps exceeding 3 cm, but is hindered by complications such as scarce donor tissue, neuroma formation, nerve distortion or dislocation, and nerve diameter mismatch.[41,42] Although nerve guiding catheters (NGCs) can bridge nerve defects, repair is almost impossible by autologous nerve transplantation. In addition, substances such as cells and neurotrophic factors must be added to provide nutrition and oxygen; however, to date, this integrated biomaterial remains elusive.[42] This highlights the inadequacy of the current reconstructive approaches for treating severe nerve injuries.

Overall, these multifaceted obstacle barriers underlie the poor efficacy of current peripheral neuropathy treatments, making most treatments palliative rather than restorative, and highlighting the urgent need for innovative approaches.

CHM Treatment and Its Limitations

CHM and its active ingredients have multifactorial advantages in treating peripheral neuropathy, including neuroprotective and anti-inflammatory effects, enhanced anti-oxidant activity, improved microenvironment, promotion of angiogenesis, improved blood circulation, as well as their abundant sources, and cost-effectiveness. The detailed mechanism and application of CHM in the treatment of peripheral neuropathy can be found in Chen's review (Figure 2).[25]

Despite the promising application prospects of CHM, its clinical translation has several pharmacological obstacles. First, oral administration has low bioavailability. For example, Salvia miltiorrhiza undergoes extensive first-pass metabolism (<10% systemic availability),[43] whereas the water solubility of hydrophobic agents, such as tanshinone IIA, can be ignored.[44] Second, non-targeted distribution leads to off-target accumulation, which wastes the dosage and has the potential to cause hepatotoxicity.[27] Third, BNB excludes large therapeutic molecules and reduces the effective nerve concentrations below the regenerative thresholds.[33] Fourth, the synergistic interactions in multi-herb formulations are compromised by physicochemical incompatibilities.[29] For example, hydrophilic paeoniflorin[45] and hydrophobic tanshinone[46] cannot coexist optimally as standard carriers. Collectively, these limitations require engineered delivery systems to unlock CHM's therapeutic potential.

Engineered Chinese Herb Delivery Systems

Nanocarriers

Nanocarriers represent a first-line strategy in our proposed framework to overcome the dual challenges of BNB impermeability and the demand for spatiotemporal precision in PN therapy. By encapsulating CHM active ingredients, these engineered systems directly address the pharmacological limitations of poor bioavailability and non-targeted distribution. Their subcellular size enables penetration of the BNB through passive diffusion or active ligand-mediated targeting, thereby ensuring sufficient drug accumulation at the nerve injury site. Furthermore, the design flexibility of nanocarriers allows for the incorporation of stimulus-responsive elements, making them uniquely capable of releasing their payload in response to specific phase-specific microenvironmental cues (eg, pH, enzymes). This capability is crucial for addressing the conflicting demands across the inflammatory, repair, and fibrotic phases of nerve recovery.

The utility of this approach is demonstrated by several encapsulation strategies designed to enhance bioavailability and stability. For instance, curcumin-loaded polycaprolactone nanofibers increased cellular uptake and extended neurite growth by 1.7-fold compared to pure polymer controls, as demonstrated in neuronal models.[47] Lycium barbarum polysaccharide (LBP) encapsulated in poly (lactic-co-glycolic acid) (PLGA) core-shell fibers achieved sustained release for over 60 days, enhancing SCs proliferation by 50%.[48] Electrospun PCL/gelatin nanofibrous scaffolds enable sustained

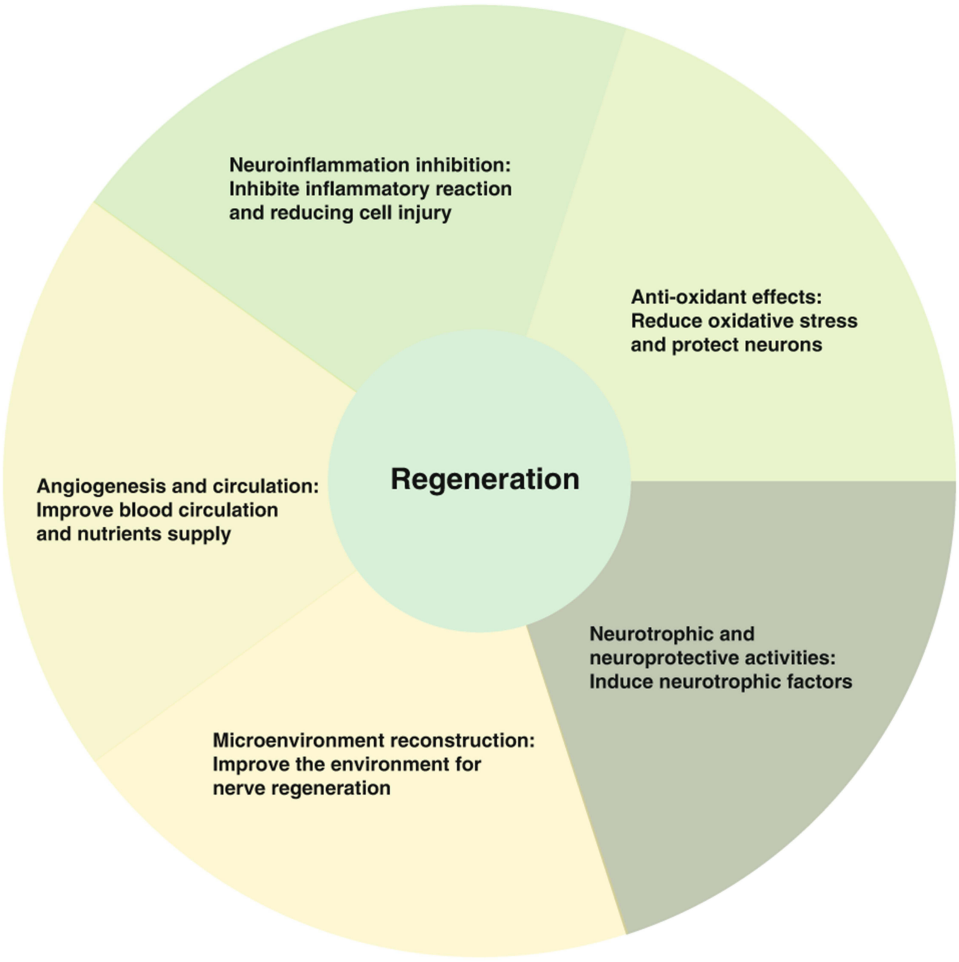

Figure 2 Mechanisms of CHM in regulating peripheral nerve repair and regeneration following PN. CHM promotes peripheral nerve regeneration after PN through various mechanisms, including: exerting anti-oxidant effects to mitigate oxidative stress and protect neurons; inhibiting neuroinflammation to suppress inflammatory reactions and reduce cellular injury; mediating neurotrophic and neuroprotective activities to induce neurotrophic factors; reconstructing the local microenvironment to optimize conditions for nerve regeneration; and promoting angiogenesis and circulation to enhance blood flow and nutrient supply.[25] Copyright 2025, Springer.

Ginkgo biloba extract (GBE) release (73.37% over 10 days), which exerts its neuro-regenerative effects through its active compounds, primarily flavonoids and terpenoids. These compounds are responsible for the observed significant reduction in pro-inflammatory cytokines (IL-6, TNF-α) via modulation of macrophage activity. When this GBE-loaded scaffold is combined with adipose-derived stem cells (ADSCs), a powerful synergy emerges. The ADSCs further contribute to immunomodulation and secrete essential neurotrophic factors. Together, this combination treatment leads to a significant upregulation of NGF and BDNF in the sciatic nerve tissue, creating a balanced inflammatory microenvironment and enhancing axonal regeneration.[49]

A key advantage of nanocarriers within our framework is their versatility in overcoming biological barriers and enabling precise intervention. They penetrate the BNB via passive diffusion,[47,48] whereas conductive components such as polyaniline-doped nanofibers reduce the charge transfer resistance to enhance ion exchange and nutrient delivery.[47] Ligand-mediated targeting strategies enhance site-specific delivery: gambogic acid-conjugated nanoparticles improve systemic bioavailability for DNP treatment,[50] while other functionalized systems achieve receptor-mediated transport to the dorsal root ganglia (DRG), reducing off-target effects in neuropathic pain models.[51,52]

This targeted capability is complemented by spatiotemporal control mechanisms. Stimuli-responsive designs allow for precise drug release aligned with pathological phases; for example, chitosan/hyaluronic acid nanoparticles released 90% payload at pH 6.14 (inflammatory phase) versus 19% payload at physiological pH.[53] Aligned electrospun

nanofibers, such as poly(3-hydroxybutyrate-co-3-hydroxyvalerate) blended with aloe vera, provide topological guidance for directional axonal regeneration.[54]

These engineered systems collectively demonstrate superior efficacy in preclinical studies, with their functional benefits supported by distinct molecular mechanisms. Conductive nanofibers upregulate neuronal differentiation markers (βIII-Tubulin 2.1-fold; TREK-1 1.8-fold) in PC12 cells.[47] Crucially, nano-curcumin formulations produce significant functional recovery by targeting specific pathological pathways: they alleviate neuropathic pain by inhibiting $P2X_3$ and $P2Y_{12}$ receptors in the DRG and suppressing associated ERK1/2 and Akt signaling,[51,52] and mitigate neuroinflammation by reducing NLRP3 expression and IL-1β maturation, alongside a ~50% reduction in macrophage infiltration.[50] Furthermore, they address oxidative stress via Nrf2 pathway activation, leading to enhanced remyelination. These actions translate to key functional outcomes, including the restoration of 85% sciatic nerve conduction velocity and a 65% increase in motor nerve conduction velocity in Charcot-Marie-Tooth (CMT) models,[55] as well as the normalization of intraepidermal nerve fiber density in DNP at half the dose of free curcumin.[50] Electrical stimulation of conductive scaffolds extended the DRG neurite length by 31%.[56] In vivo, PLGA-LBP scaffolds promoted neurite extension for 3.4-fold longer than non-engineered groups[48] (Table 1 and Table 2).

Despite these advances, its clinical translation has faced significant hurdles. Scalability issues arise from batch inconsistencies in coaxial electrospinning, where fiber diameter variations (295–896 nm) compromise drug release consistency.[48] Biocompatibility concerns include inflammatory responses triggered by acidic degradation byproducts of conductive polymers[73] and unassessed chronic toxicity of metallic nanoparticles.[74] Dosage optimization remains challenging, as high LBP concentrations reduce scaffold tensile strength by 22%,[48] whereas industrial processing diminishes bioactive components such as aloe vera polysaccharides.[54] Targeting precision requires refinement to prevent off-target effects,[51,52] and regulatory pathways lack standardization for nanocarrier characterization in large-animal models.[49,51]

The compelling evidence for BNB penetration, targeted delivery, and spatiotemporal control, as summarized in this section, is exclusively in preclinical investigations. The hypothesis that nanocarriers can serve as a primary strategy to overcome pharmacological barriers in human PN patients awaits validation in clinical settings.

Hydrogels

Within our therapeutic framework, hydrogels emerge as a uniquely suited platform for tackling the challenge of microenvironmental imbalance in PN. Their fundamental advantage lies in the use of biocompatible natural polymers that undergo synchronous degradation with the native process of nerve regeneration. For instance, alginate/chitosan hydrogels demonstrate principle by losing approximately 80% of their mass over 14 days, a timeline that aligns with key phases of peripheral nerve repair.[57] This timed degradation is designed to supply sustained support throughout the vulnerable regeneration phase.

The functional capacity of hydrogels is significantly advanced by engineering complex stimuli-responsive systems that enable spatiotemporally precise drug release. This design directly addresses the dynamic pathological shifts in PN. NIR-activated curcumin hydrogels utilize π-π stacking with synthetic melanin nanoparticles to achieve on-demand payload release,[58] whereas collagen-based hydrogels loaded with naringin deliver an initial 22.5% burst release within 12 h for acute inflammation control,[59] followed by sustained delivery of 72.5% over 14 days to support chronic regeneration.[59] Conductive hydrogels incorporating reduced graphene oxide exhibit electrical conductivity of 5.27×10^{-4} S/cm, enhancing neural differentiation under electrostimulation.[71] Multifunctional designs combine drug delivery with auxiliary therapies: supramolecular hydrogels co-deliver ginsenoside Rg1, Stromal cell-derived factor-1α (SDF-1α), and stem cells to synergistically regulate neurogenesis and angiogenesis,[60] whereas boronic ester-based hydrogels enable long-term curcumin release (71.4% over 28 days) via dual cross-linking.[61]

A pivotal function of hydrogel systems is their ability to simultaneously overcome CHM bioavailability issues and actively correct the dysregulated microenvironment. For hydrophobic compounds like curcumin, encapsulation in lipid nanocapsules achieves 92.7% efficiency,[62] whereas berberine and naringin nanoparticles in chitosan/alginate matrices improved solubility by 51.6% and 47.1%, respectively.[63] Porous architectures with pore dimensions of 22–32 μm in chitosan/alginate hydrogels,[63] 50–250 μm in chitosan/oxidized cellulose composites,[71] and 90 μm in collagen scaffolds[59]

Table 1 Comprehensive Summary of in vivo Animal Studies on Engineered CHM Delivery Systems for PN

PN Model	CHM Compound/ Formula	Carrier Type/Size/Load	Route/Dose	Comparators	Main Outcomes	Safety Signals	References
Rat sciatic nerve transection	Ginkgo biloba extract (GBE)	**Type**: Electrospun PCL/gelatin nanofibrous scaffold. Average Fiber **Size**: ~634.69 ± 192.65 nm (GBE-loaded), ~578.3 ± 119.22 nm (GBE-free). **Load**: 10 v/v% GBE.	**Route**: Implantation of the neural conduit at the injury site. **Dose**: The conduit was seeded with 50,000 ADSCs in 1.5 wt.% collagen hydrogel.	1. Autograft group 2. GBEPCLGELADSCs + Physical Activity group 3. GBEPCLGELADSCs group (without PA) 4. PCLGEL + Physical Activity group 5. PCLGEL group (without PA) 6. Negative Control group (no treatment)	1. GBE Release: ~73% cumulative release over 10 days. 2. Anti-inflammatory: GBE scaffolds significantly reduced pro-inflammatory cytokines (IL-6, TNF-α) vs controls. 3. Functional Recovery (vs other experimental groups): The GBEPCLGELADSCs + PA group showed: Significantly higher SFI at 8 weeks; Significantly lower gastrocnemius muscle weight loss (~comparable to autograft); Significantly shorter hot plate latency. 4. Neurotrophic Factors: Significantly higher NGF & BDNF levels vs all other groups except autograft.	The developed PCL/Gelatin scaffolds, both with and without GBE, showed no cytotoxicity to PC-12 cells, confirming their biocompatibility. No adverse safety signals were reported.	[49]
Rat diabetic neuropathy	Curcumin	**Type**: PLGA-GA_2 double-headed nanoparticles (nCUR). **Size**: ~270 nm (PDI ~0.25). **Load**: 0.112 mg of Curcumin per mg of PLGA-GA_2 polymer.	Oral, 20 mg CUR equivalent/kg/day.	1. Control (Non-diabetic) 2. Diabetic (D) 3. D + Curcumin (40 mg/kg/day, oral) 4. D + nCUR 5. D + nCUR + Insulin 6. D + Insulin	1. Nerve Fiber Density: nCUR and nCUR+ Insulin groups showed ~2 to 3-fold higher intraepidermal nerve fiber density and Bielschowsky-stained axonal neurites compared to the diabetic group. 2. Cell Death: nCUR+ Insulin treatment reduced TUNEL-positive cells by ~60-70% vs the diabetic group. 3. Inflammation: nCUR and nCUR+ Insulin significantly reduced mRNA levels of NLRP3 (~70-80% decrease) and IL-1β (~60-70% decrease) in the sciatic nerve and spinal cord. 4. Macrophage/T-cell Infiltration: nCUR+ Insulin reduced F4/80+ macrophage infiltration by ~50% and CD3+ T-cell infiltration by ~40% in the sciatic nerve. 5. Functional Preservation: nCUR and nCUR+ Insulin preserved hind paw pad area and NF200 expression, comparable to non-diabetic controls	The nCUR formulation was reported as safe based on prior studies with similar polymers. No direct toxicity or adverse events were reported in this study.	[50]

HIV-gp120-induced neuropathic pain in rat	Curcumin	**Type**: Poly (PEGMA-DMAEMA-MAO) nanoparticles/microspheres. **Size**: Information not explicitly stated for the final loaded microspheres. The freeze-dried nano-curcumin precursor had an average size of ~270 nm. **Load**: Prepared from a solution of 50 mg Curcumin and 60 mg Poly-PEGMA-DMAEMA-MAO polymer.	**Route**: Intravenous (via sublingual vein injection). **Dose**: Nanoparticle-encapsulated curcumin at a concentration of 4 mg/mL (specific volume per rat not detailed).	1. Control group (Ctrl) 2. Sham operation group (Sham) 3. HIV-gp120 group (gp120) 4. HIV-gp120 + Nano Curcumin group (gp120 + nano curcumin) 5. HIV-gp120 + Nano Carrier group (gp120 + nano carrier)	1. Pain Behavior: Nano-curcumin significantly increased the Mechanical Withdrawal Thresholdand Thermal Withdrawal Latency in gp120-treated rats, reversing the hyperalgesia. The effects were statistically significant ($p < 0.01$) from days 7–14 post-surgery. 2. Molecular Expression: Nano-curcumin significantly decreased gp120-induced upregulation of P2X3 mRNA and protein expression in DRG ($p < 0.01$). 3. Signaling Pathway: Nano-curcumin significantly reduced gp120-induced phosphorylation of ERK1/2 (p-ERK1/2) in DRG ($p < 0.01$). 4. Electrophysiology: Nano-curcumin (0.2 μg/mL) significantly decreased the P2X3 agonist (α, β-me-ATP)-induced currents in DRG neurons cultured with gp120 ($p < 0.01$).	The nanoparticle encapsulation carrier alone (gp120 + nano carrier group) did not show significant effects on pain behavior or molecular markers compared to the gp120-only group, suggesting the carrier itself did not induce obvious adverse effects or toxicity in this model. No other toxicity was reported.	[51]
Type 2 diabetic neuropathic pain model in rats induced by high-fat diet and intraperitoneal injection of streptozotocin.	Curcumin	**Type**: Poly-PEGMA-DMAEMA-MAO nanoparticles; **Load**: 25% curcumin; **Size**: Not specified in the study.	**Route**: Sublingual vein injection; **Dose**: 16 mg/kg nanoparticle-encapsulated curcumin (equivalent to 4 mg/kg curcumin) twice in the 7th and 8th weeks.	1. Control group (conventional diet, citrate buffer injection) 2. DM group (diabetic, untreated) 3. DM + nano carrier group (carrier without curcumin)	1. Behavioral Pain: Nano-curcumin significantly increased the Mechanical Withdrawal Threshold and Thermal Withdrawal Latency at the 10th week compared to the DM group ($p < 0.01$). 2. P2Y12 Receptor: mRNA and protein expression, which were upregulated in DM rats, were significantly decreased by nano-curcumin treatment ($p < 0.01$). 3. Inflammation & Glial Activation: IL-1β and Connexin43 (Cx43) mRNA and protein expression were significantly lower in the nano-curcumin group vs the DM group ($p < 0.01$). 4. Signaling Pathway: The p-Akt/Akt ratio was significantly reduced in the nano-curcumin group compared to the DM group ($p < 0.01$). 5. Blood Glucose: Nano-curcumin treatment reduced blood glucose from 15.34 ± 0.84 mmol/L (7 w) to 12.01 ± 0.93 mmol/L (10 w) ($p < 0.05$ vs DM group which remained at ~14.8 mmol/L).	No significant adverse effects reported; blood glucose levels decreased in treated groups, with no notable changes in body weight compared to diabetic controls.	[52]

(*Continued*)

https://doi.org/10.2147/DDDT.S563805

Table 1 (Continued).

PN Model	CHM Compound/ Formula	Carrier Type/Size/Load	Route/Dose	Comparators	Main Outcomes	Safety Signals	References
Rat CMT1A model	Curcumin	**Type**: Curcumin-cyclodextrin/cellulose nanocrystals (Nano-Cur). Curcumin is incorporated into the hydrophobic cavity of β-cyclodextrin (β-CD) bound to cellulose nanocrystal (CNCx) surfaces. **Size**: CNCx have a uniform nanorod shape: 100–200 nm long, 10–20 nm wide, and 5–10 nm thick. **Load**: Not explicitly specified in the provided text.	**Route**: Intraperitoneal injection. **Dose**: 0.2 mg/kg/day of curcumin (delivered via Nano-Cur) for 8 weeks.	1. WT rats treated with saline (WT/Saline) 2. WT rats treated with the nanoparticle carrier (CD/CNCx) alone (WT/Nano) 3. WT rats treated with Nano-Cur (WT/Nano-Cur) 4. CMT1A rats treated with saline (CMT1A/Saline) 5. CMT1A rats treated with the nanoparticle carrier (CD/CNCx) alone (CMT1A/Nano)	1. Motor Nerve Conduction Velocity: Increased by ~77% in CMT1A/Nano-Cur rats (25.0 m/s) compared to CMT1A/Saline controls (14.1 m/s). (WT: ~40 m/s) 2. Compound Muscle Action Potential: Increased by ~188% in CMT1A/Nano-Cur rats (7.2 mV) compared to CMT1A/Saline controls (2.5 mV). (WT: ~15 mV) 3. Sensory Nerve Conduction Velocity: Restored to a measurable 12.5 m/s in CMT1A/Nano-Cur rats, where it was undetectable in untreated CMT1A controls. (WT: ~36 m/s) 4. Myelin Thickness: Increased by ~34% in CMT1A/Nano-Cur rats (1.18 μm) compared to CMT1A/Saline controls (0.88 μm). (WT: ~2.05 μm) 5. G-ratio: Reduced by ~10% in CMT1A/Nano-Cur rats (0.64) compared to CMT1A/Saline controls (0.71), indicating improved myelination. (WT: ~0.57) 6. ROS in Sciatic Nerve: Significantly reduced to levels similar to the WT/Saline group. 7. Nrf2 Protein: Expression increased by ~49% in CMT1A/Nano-Cur rats compared to CMT1A/Saline controls. 8. Creatine Phosphokinase: Plasma levels in CMT1A/Nano-Cur rats were normalized and showed no significant difference from WT/Saline levels, unlike the elevated levels in untreated CMT1A controls.	No adverse effects reported. Well-tolerated with no safety concerns. Nanoparticle carrier alone showed no negative effects.	[55]

Rat sciatic nerve crush	Hesperidin	**Type**: Alginate/Chitosan (Alg/Chit) hydrogel. **Pore Size**: ~75 μm. **Porosity**: ~90%. **Load**: Hesperidin loaded at 0.1%, 1%, and 10% (w/v).	**Route**: Local injection at the sciatic nerve crush site. **Dose**: 0.3 mL of hydrogel containing a specific concentration of hesperidin (0.1%, 1%, or 10% w/v).	1. Negative Control (Injury, no treatment) 2. Positive Control (No injury) 3. Alg/Chit Hydrogel (Hesperidin 0%) 4. Alg/Chit/0.1% Hesperidin 5. Alg/Chit/10% Hesperidin	1. SFI: The Alg/Chit/1%Hes group showed an SFI of −17.80 ± 2.65 at 8 weeks, significantly better than the negative control (−80.8 ± 1.12) and the empty hydrogel group (−59.13 ± 4.08). 2. Hot Plate Latency: The Alg/Chit/1%Hes group had a latency of 4.33 ± 0.57s, close to the positive control (3.66 ± 1.15s) and significantly better than the negative control (~12s, cutoff). 3. Muscle Weight Loss: The Alg/Chit/1%Hes group had the lowest gastrocnemius muscle wet weight loss (0.19 ± 0.03%), significantly better than the negative control. 4. Histology: The Alg/Chit/1%Hes group showed nerve and muscle fiber structure most similar to the normal group, with well-arranged myelinated fibers and minimal vacuolation/fibrosis.	No toxicity or negative effects on cell viability. Excellent blood compatibility (low hemolysis). Demonstrated antibacterial properties. All hydrogels were well-tolerated.	[57]
Sciatic nerve crush injury in rat	Curcumin	**Type**: Curcumin loaded in artificial allmelanin nanoparticles (AMNP@Cur) within a conductive hydrogel composed of polyaniline-grafted quaternized chitosan (PQCS) and oxidized dextran (OD), termed PQCD-A@Cur. **Size**: AMNP ~130 nm (SEM/TEM); AMNP@Cur hydrodynamic diameter ~172.83 ± 1.72 nm. **Load**: Curcumin loading ratio of 24.4% at 1 mg/mL Cur concentration and 27.3% at 2 mg/mL.	**Route**: Local perineural injection for nerve injury; topical application/ subcutaneous injection for diabetic wounds. **Dose**: 50 μL hydrogel for nerve injury (containing ~0.067 mg Cur per mL hydrogel, thus ~0.00335 mg Cur per 50 μL); 300 μL hydrogel for diabetic wounds.	Sham, Crush (or Control), PQCD, PQCD-A, PQCD-A@Cur, PQCD-A + NIR, PQCD-A@Cur + NIR.	1. The PQCD-A@Cur + NIR group showed a myelin sheath thickness of 360.00 nm, significantly greater than the Crush group (104.67 nm). 2. The myelinated axon density was significantly higher in the PQCD-A@Cur + NIR group compared to the Crush group. 3. At 4 weeks, the PQCD-A@Cur + NIR group showed a swing time of 104.00% (of contralateral side), significantly better than the Crush group (134.67%). 4. The muscle weight ratio of the injured limb was 88.49 in the PQCD-A@Cur + NIR group, significantly higher than the Crush group (62.49). 5. The PQCD-A@Cur + NIR group significantly reduced the fluorescence intensity of pro-inflammatory cytokines (IL-6, TNF-α) and enhanced the anti-inflammatory cytokine IL-10 compared to the Crush group.	**In Vitro**: No significant cytotoxicity; cell viability >95% in all groups. **In Vivo**: No abnormalities or inflammatory infiltration in vital organs (heart, liver, spleen, kidney) after 10 days.	[58]

(*Continued*)

Table 1 (Continued).

PN Model	CHM Compound/ Formula	Carrier Type/Size/Load	Route/Dose	Comparators	Main Outcomes	Safety Signals	References
Rat sciatic nerve crush	Naringin	**Type**: Collagen Type I Hydrogel. **Size**: Average pore size of 90 ± 5 μm. **Load**: Naringin:Collagen weight ratio of 1:10.	**Route**: Local injection into the injury site. **Dose**: 50 μL of hydrogel.	1. Negative Control (Injury, no treatment) 2. Pure Collagen Hydrogel 3. Positive Control (Autograft)	1. Functional Recovery: The Collagen/Naringin group showed an SFI of −22.13 ± 3.00 at 60 days, significantly better than the Negative Control (−82.60 ± 1.06) and the Pure Collagen group (−59.80 ± 3.20). 2. Electrophysiology: The Collagen/Naringin group had a CMAP amplitude of 22.32 ± 1.60 mV, significantly higher than the Negative Control (5.72 ± 1.45 mV) and the Pure Collagen group (10.70 ± 2.05 mV). 3. Muscle Atrophy: The Collagen/Naringin group showed a gastrocnemius muscle wet weight loss of 5.7 ± 1.3%, significantly lower than the Negative Control and the Pure Collagen group (9.1 ± 1.3%). 4. Sensory Recovery (Hot Plate Latency): The Collagen/Naringin group had a latency of 6.00 ± 0.81 s, significantly better than the Negative Control (which did not react within 12s) and the Pure Collagen group (~9s).	**In Vitro Cytocompatibility**: The Collagen/Naringin hydrogel significantly promoted Schwann cell proliferation with no cytotoxicity. **Hemocompatibility**: The Collagen/Naringin hydrogel induced negligible hemolysis, which was significantly lower than the positive control (water).	[59]
Diabetic mouse wound model	Ginsenoside Rg1, SDF-1α	**Type**: Anionic liposomes (DSPC, DSPG, Cholesterol). **Size**: ~146.1 nm in diameter. **Load**: Encapsulation Efficiency: SDF-1α 86.4%, Rg1 95.2%. Final concentrations in hydrogel: SDF-1α ~5 μg/mL, Rg1 ~400 μg/mL.	**Route**: Local subcutaneous injection around the wound site. **Dose**: 100 μL of the composite hydrogel.	1. Control (PBS) 2. Gel (Hydrogel only) 3. Gel@LipoSDF&RG1 (Hydrogel + Drug-loaded liposomes) 4. Gel@LipoSDF&RG1/ADSCs (Hydrogel + Drug-loaded liposomes + ADSCs)	1. Wound Closure: The Gel@LipoSDF&RG1/ADSCs group showed a wound closure rate of approximately 95% at day 14, significantly higher than the Control group (~40%) and the Gel group (~55%). 2. Angiogenesis: The number of CD31+ blood vessels was highest in the Gel@LipoSDF&RG1/ADSCs group (~25 vessels/field), significantly greater than the Control group (~5 vessels/field). 3. Macrophage Polarization: The Gel@LipoSDF&RG1/ADSCs group significantly increased the proportion of M2 macrophages and decreased M1 macrophages, with the M2/M1 ratio being the highest among all groups. 4. Nerve Regeneration: Expression of neural markers Nestin and β3-tubulin was significantly higher in the Gel@LipoSDF&RG1 and Gel@LipoSDF&RG1/ADSCs groups compared to the Control and Gel-only groups. 5. Collagen Deposition: The Gel@LipoSDF&RG1/ADSCs group showed the most significant collagen deposition in Masson's trichrome staining.	**In Vitro Biocompatibility**: The hydrogel showed low cytotoxicity and excellent biocompatibility with ADSCs, maintaining high cell viability before and after injection. **In Vivo Biocompatibility**: H&E staining of major organs (heart, liver, spleen, lung, kidney) from treated mice showed no notable tissue damage or signs of toxicity compared to the control group.	[60]

Mouse sciatic nerve chronic constriction injury	Curcumin	**Type**: Curcumin (Cur) encapsulated in thiolated Pluronic F127 micelles (Cur-M) and incorporated into a boronic ester-based dynamic hydrogel (Gel-Cur-M). **Size**: Cur-M diameter: ~33.68 ± 0.83 nm (for 50:1 ratio), PDI: 0.34 ± 0.03. **Load**: Cur encapsulation efficiency: up to 92.68 ± 4.33% (for 50:1 ratio); Cur loading efficiency: up to 7.86 ± 0.68% (for 50:5 ratio).	**Route**: Orthotopic injection around the injured sciatic nerve; **dose**: 30 μL of Cur-M, Gel, or Gel-Cur-M (equivalent Cur concentration based on formulation).	Sham (nerve exposure only), CCI (no treatment), Cur-M alone, Gel alone, Gel-Cur-M.	1. Mechanical allodynia: Gel-Cur-M increased withdrawal threshold to ~2.0 g vs CCI (~0.5 g). 2. Thermal hyperalgesia: Gel-Cur-M increased withdrawal latency to ~12 s vs CCI (~6 s). 3. Pressure ratio (Ipsilateral/Contralateral): Gel-Cur-M restored to ~1.0 (similar to Sham). 4. Stance/Swing duration: Gel-Cur-M significantly improved coordination vs CCI. 5. Gastrocnemius wet weight: Gel-Cur-M preserved muscle mass (~120 mg vs CCI ~80 mg). 6. Contractile force: Gel-Cur-M improved force to ~1.2 N vs CCI (~0.8 N). 7. Macrophage density and TNF-α area: Gel-Cur-M reduced by ~50-70% vs CCI. 8. Axon & Myelin area: Gel-Cur-M preserved structural integrity (~15 μm² and ~10 μm² vs CCI ~10 μm² and ~5 μm²). 9. TRPV1 in DRG: Gel-Cur-M reduced expression by ~50%.10. Microglial activation (IBA-1): Gel-Cur-M reduced area ratio to ~1.2 vs CCI (~2.0). 11. Tnf, Csf1, Ccl2, Trpv1: Gel-Cur-M caused 2- to 3-fold decrease vs CCI.	No cytotoxicity in vitro: Cur up to 10 μM safe for rat Schwann cells; Cur-M and Gel-Cur-M showed no cytotoxicity in MTT assay. No adverse effects reported in vivo; hydrogel components are biocompatible and degradable.	[61]
Rat chronic constriction injury	Curcumin (Cur)	**Type**: Lipid Nanocapsules (LNCs) incorporated into an injectable hydrogel (0.3 GC polymer crosslinked with HRP/H_2O_2). **Size**: Cur@LNCs diameter ~100 nm (from DLS and TEM). **Load**: Encapsulation Efficiency up to 95% (for 1.0% drug load); Drug Loading up to 1.79% (wt/wt) (for 2.0% drug load).	**Route**: Intramuscular injection at the injury site; **dose**: 400 μL per rat (containing 0.3 GC + Cur@LNCs).	1. Untreated (CCI only) 2. Free LNC hydrogel (0.3 GC + LNCs) 3. Curcumin-loaded LNC hydrogel (0.3 GC + Cur@LNCs)	1. Thermal Hyperalgesia): Cur@LNCs group showed a significant reduction in pain, returning to baseline levels within 7 days post-administration. 2. H&E: The H&E score was significantly higher in the 0.3 GC + Cur@LNCs group compared to both the untreated control ($P < 0.05$) and the free LNC group ($P < 0.05$).	No acute systemic toxicity or nerve injury observed at the injection site in the 0.3 GC + Cur@LNCs group. The Cur@LNCs hydrogel group showed significantly reduced tissue damage and fewer infiltrating lymphocytes compared to other groups.	[62]
Rat sciatic nerve crush	Berberine and Naringin	**Type**: Chitosan/Alginate hydrogel composited with Berberine and Naringin-loaded Chitosan Nanoparticles. **Size**: Ber-NPs: 594 nm; Nar-NPs: 636 nm. **Load**: Ber EE: 51.6 ± 7.4%; Nar EE: 47.1 ± 5.8%.	**Route**: Injection into the lesion site; **dose**: 0.3 mL of hydrogel.	1. Negative Control (Injury, no treatment) 2. Positive Control (No injury) 3. Cs/Alg Hydrogel 4. Cs/Alg/Ber Hydrogel 5. Cs/Alg/Nar Hydrogel 6. Cs/Alg/Ber/Nar Hydrogel	1. Motor Function (SFI): Cs/Alg/Ber/Nar group showed near-complete recovery (SFI ≈ −14.6 at 8 weeks) vs Negative Control (SFI ≈ −80). 2. Sensory Function (Hot Plate Latency): Cs/Alg/Ber/Nar reduced latency to 4.66 ± 0.57 s vs Negative Control (~12 s cutoff). 3. Muscle Atrophy (Weight Loss): Cs/Alg/Ber/Nar significantly reduced weight loss to ~20% vs Negative Control (~50%). 4. Muscle Morphology (Cross-Sectional Area): Cs/Alg/Ber/Nar resulted in a CSA of 2219 ± 107 μm², similar to the Positive Control. 5. Cell Proliferation (MTT Assay): Cs/Alg/Ber/Nar hydrogel showed the highest cell proliferation on PC12 cells at 72h.	**Hemocompatibility**: Hemolysis rates for all hydrogels were below 5%, meeting ASTM standards. **Biocompatibility**: All prepared hydrogels showed no cytotoxic effects and supported PC12 cell viability and proliferation.	[63]

(*Continued*)

Table 1 (Continued).

PN Model	CHM Compound/ Formula	Carrier Type/Size/Load	Route/Dose	Comparators	Main Outcomes	Safety Signals	References
Rat sciatic nerve crush	Berberine	**Type**: Alginate/Chitosan hydrogel. **Size**: Average pore size of 38.2 ± 11 μm (without Ber) and 40 ± 9.5 μm (with 10% Ber). **Load**: Loaded with 0%, 0.1%, 1%, or 10% (w/w) Berberine.	**Route**: Injection around the injured sciatic nerve; **dose**: 0.4 mL of hydrogel.	1. Negative Control (Injury, no treatment) 2. Positive Control (No injury) 3. Alg/Chit Hydrogel (0% Ber) 4. Alg/Chit/0.1% Ber 5. Alg/Chit/1% Ber 6. Alg/Chit/10% Ber	1. Motor Function (SFI): Alg/Chit/1%Ber group showed significant recovery (SFI = −20.23 ± 1.35) vs Negative Control (SFI = −76.90 ± 4.12). 2. Sensory Function (Hot Plate Latency): Alg/Chit/1%Ber group had a latency of 5 ± 1 s vs Negative Control (no response at 12s cutoff). 3. Muscle Atrophy (Weight Loss): Alg/Chit/1% Ber group showed the lowest weight loss (9.91 ± 2.61%) vs Negative Control. 4. Muscle Morphology (Cross-Sectional Area): The Alg/Chit/1%Ber group had a CSA closest to the Positive Control. 5. Drug Release: Sustained release profile with ~90% of Berberine released over 24 days.	**Hemocompatibility**: All hydrogels showed hemolysis rates significantly lower than the positive control, confirming blood compatibility. **Cytocompatibility**: All hydrogels were cytocompatible and supported PC12 cell proliferation. A dose-dependent effect was observed, with 1% Ber showing the highest proliferation and 10% Ber showing reduced proliferation due to cytotoxicity.	[64]
Rat sciatic nerve crush	Curcumin	**Type**: Keratin/Chitosan hydrogel (C/K = 1:1), **size**: 8×5 × 1.5 mm^3, **load**: 500 μg curcumin	**Route**: Local implantation around the crushed nerve, **Dose**: single dose of 500 μg curcumin	Sham, Control (crush only), C/K hydrogel, Curcumin only, C/K/C hydrogel	1. SFI: CKC group > Cur and CK groups > Control (eg, CKC SFI at 4 weeks: −47.6 vs Control: −72.4) 2. Muscle weight: CKC group significantly higher than Control ($P < 0.05$) 3. CMAP amplitude: CKC > Cur > CK > Control (eg, CKC: ~45 mV vs Control: ~20 mV) 4. Nerve conduction velocity: CKC > Cur > CK > Control (eg, CKC: ~41.2 m/s vs Control: ~30.1 m/s) 5. Axon count: CKC > CK and Cur > Control (eg, CKC: ~450 axons/field vs Control: ~200 axons/field) 6. Myelin thickness: CKC > CK and Cur > Control (eg, CKC: ~0.8 μm vs Control: ~0.4 μm)	No significant inflammatory response, no organ injury, no systemic toxicity, good biocompatibility and degradability	[65]

Rat sciatic nerve transection	Curcumin	**Type**: Chitosan/Polyethylene oxide biodegradable membrane, **size**: 1×1 cm, **load**: Not specified (used as a physical scaffold)	**Route**: Intraperitoneal injection of curcumin at 100 mg/kg/day for 4 weeks; **Dose**: membrane applied locally around the transected nerve	Control (sutured only), Curcumin only, Membrane only, Membrane + Curcumin	1. SFI at 8 weeks: Mem+Cur: −64.90 ± 5.07; Mem: −71.88 ± 3.32; Cur: −75.28 ± 5.23; Ctrl: −78.48 ± 0.88 2. WRL at 8 weeks (s): Mem+Cur: 3.07 ± 1.14; Mem: 4.66 ± 0.58; Cur: 5.48 ± 1.29; Ctrl: 5.64 ± 1.90 3. EMG Amplitude (mV): Mem+Cur: 5.34 ± 1.82; Mem: 5.34 ± 1.81; Cur: 4.14 ± 2.42; Ctrl: 3.57 ± 0.53 4. EMG Latency (ms): Mem+Cur: 1.82 ± 0.19; Mem: 2.54 ± 0.53; Cur: 2.40 ± 0.38; Ctrl: 2.53 ± 0.27 5. Nerve Fiber Count: Mem+Cur: 46.66 ± 7.42; Mem: 47.08 ± 1.78; Cur: 46.08 ± 6.94; Ctrl: 38.08 ± 3.38 6. Myelin Thickness (μm): Mem+Cur: 2.19 ± 0.69; Mem: 2.98 ± 0.49; Cur: 2.21 ± 0.32; Ctrl: 1.67 ± 0.60	No adverse events or safety issues reported; good biocompatibility of chitosan membrane and no systemic toxicity observed with curcumin administration	[66]
Rat cavernous nerve injury	Curcumin	**Type**: PLGA-PEG slow-release membrane (thickness: 0.5 mm, **size**: 5×5 mm or 10×10 mm). **Load**: 0.35%, 0.7%, 1.4% curcumin (w/w). Drug loading: 3.49 ± 0.06, 7.06 ± 0.12, 13.89 ± 0.17 μg/mg. Encapsulation rate: ~93%.	**Route**: Local implantation next to the injured cavernous nerve. Doses correspond to 0.35%, 0.7%, and 1.4% curcumin-loaded membranes.	Sham, BCNC (nerve injury only), Blank membrane (PLGA-PEG without curcumin), Low/Medium/ High-dose CUR membrane groups	1. ICP/MAP Ratio: Sham: 0.82 ± 0.05; High-dose: 0.68 ± 0.07; Medium-dose: 0.64 ± 0.07; Low-dose: 0.51 ± 0.05; Blank: 0.34 ± 0.07; BCNC: 0.32 ± 0.06 2. Myelinated Nerve Fiber Count: Sham: 209.50 ± 7.99; High-dose: 157.17 ± 9.35; Medium-dose: 126.50 ± 12.24; Low-dose: 87.67 ± 10.54; Blank: 46.83 ± 5.42; BCNC: 47.50 ± 5.89 3. Smooth Muscle/Collagen Ratio: Sham: 0.36 ± 0.03; High-dose: 0.29 ± 0.06; Medium-dose: 0.25 ± 0.05; Low-dose: 0.23 ± 0.02; Blank: 0.19 ± 0.04; BCNC: 0.20 ± 0.03 4. nNOS Protein & mRNA: Significantly increased in CUR groups vs BCNC/Blank ($P < 0.05$), dose-dependent increase 5. Collagen-I Protein: Decreased in CUR groups vs BCNC/Blank ($P < 0.05$)	No reported toxicity or adverse events. PLGA-PEG membrane showed good biocompatibility, degradability (>85% in 10 weeks in vitro), and no significant inflammatory response.	[67]

(*Continued*)

https://doi.org/10.2147/DDDT.S563805

Table 1 (Continued).

PN Model	CHM Compound/ Formula	Carrier Type/Size/Load	Route/Dose	Comparators	Main Outcomes	Safety Signals	References
Rat common peroneal and tibial nerve transection	Modified Formula Radix Hedysari (MFRH)	Chitosan-based chitin conduit with different inner diameters at both ends (thinner end: 0.8 mm, thicker end: 1.8 mm). No drug load; used as a physical scaffold for nerve guidance.	**Route**: Oral gavage; **Dose**: MFRH at 2 mL/day (concentration: 1 g/mL) for 16 weeks post-surgery.	Sham group (exposure only), Saline group (negative control), Mecobalamin group (positive control, 100 μg/kg, 2 mL/day).	1. SFI: MFRH: ~ −55; Mecobalamin: ~ −55; Saline: ~ −70; Sham: ~ −5 2. CMAP Amplitude (mV): MFRH & Mecobalamin significantly higher than Saline ($P<0.01$), but lower than Sham ($P<0.001$). No significant difference between MFRH and Mecobalamin. 3. Myelinated Nerve Fiber Count: MFRH & Mecobalamin > Saline & Sham ($P<0.001$) 4. Axon Diameter (μm): MFRH & Mecobalamin > Saline ($P<0.01$), but < Sham ($P<0.001$) 5. Myelin Sheath Thickness (μm): MFRH & Mecobalamin > Saline ($P<0.01$), but < Sham ($P<0.01$) 6. Gastrocnemius Wet Weight Ratio: MFRH & Mecobalamin > Saline ($P<0.001$), but < Sham ($P<0.001$) 7. FG-labeled Motor Neurons: MFRH & Mecobalamin > Saline ($P<0.05$), but < Sham ($P<0.001$) 8. FG-labeled Sensory Neurons: MFRH & Mecobalamin > Saline ($P<0.05$), but < Sham ($P<0.01$)	No apparent inflammation or neuroma at the suture site. Conduit showed good biocompatibility, partial absorption by 16 weeks, and no reported adverse events from MFRH administration.	[68]

Rat sciatic nerve defect	Gastrodin	Type: Polyurethane (PU) nerve guidance conduit (NGC); Inner diameter: 1.28 mm, Outer diameter: 2.8 mm; Gastrodin loading: 0%, 1%, and 5% by weight	**Route**: Implanted as a conduit bridging a 10 mm sciatic nerve defect; **Dose**: Gastrodin released sustainably over 6 weeks	Autograft, PU conduit (0% Gastrodin), 1% Gastrodin/PU conduit	1. SFI: Autograft: ~ −25; 5% Gastrodin/PU: ~ −35.6; 1% Gastrodin/PU: ~ −48; PU: ~ −55.2. The 5% Gastrodin/PU group was significantly higher than the PU and 1% Gastrodin/PU groups ($P<0.05$). 2. CMAP Amplitude (mV): Autograft: ~ 30; 5% Gastrodin/PU: ~ 25.3; 1% Gastrodin/PU: ~ 18.5; PU: ~ 12.1. The 5% Gastrodin/PU group was significantly better than the 1% Gastrodin/PU and PU groups ($P<0.05$), but inferior to the Autograft ($P<0.05$). 3. Myelin Sheath Thickness (μm): Autograft: ~ 1.5; 5% Gastrodin/PU: ~ 1.2; 1% Gastrodin/PU: ~ 0.9; PU: ~ 0.6. The 5% Gastrodin/PU group was significantly thicker than the 1% Gastrodin/PU and PU groups ($P<0.001$). 4. Gastrocnemius Muscle Wet Weight Ratio (%): Autograft: ~ 95; 5% Gastrodin/PU: ~ 80; 1% Gastrodin/PU: ~ 70; PU: ~ 60. The 5% Gastrodin/PU group was significantly higher than the 1% Gastrodin/PU and PU groups ($P<0.01$). 5. Neurite Outgrowth (PC12 cells): The average neurite length and percentage of differentiated cells were significantly higher in the 5% Gastrodin/PU/SCs conditioned medium group compared to the 1% Gastrodin/PU and PU groups ($P<0.0001$). 6. Gene/Protein Expression: The 5% Gastrodin/PU group showed significantly higher expression of GDNF, BDNF, EGR2, and NGF, and lower expression of NCAM and TNF-α, compared to the 1% Gastrodin/PU and PU groups ($P<0.05$).	No significant systemic toxicity was observed. There was only a mild decrease in creatinine levels. The 5% Gastrodin/PU group also showed reduced fibrous capsule formation and inflammation, indicating good biocompatibility.	[69]

(*Continued*)

https://doi.org/10.2147/DDDT.S563805

Table 1 (Continued).

PN Model	CHM Compound/ Formula	Carrier Type/Size/Load	Route/Dose	Comparators	Main Outcomes	Safety Signals	References
Rat sciatic nerve injury	Berberine	Polyacrylonitrile/Chitosan (PAN/CS) nanofibrous conduit; Average fiber diameter: ~245 nm; Berberine administered orally, not loaded in the conduit.	**Route**: Oral administration in drinking water; **Daily dose**: 30 mg per rat for 8 weeks.	1. Scaffold/Cells/Berberine 2. Scaffold/Cells 3. Scaffold 4. Berberine 5. Control (untreated injury)	1. SFI (8 weeks): Scaffold/Cells/Berberine: −24.08; Scaffold/Cells: −25.35; Scaffold: −31.59; Berberine: −36.84; Control: −39.27. The Scaffold/Cells/Berberine group showed the most significant functional recovery, closely followed by the Scaffold/Cells group. 2. Nerve Diameter (μm): Scaffold/Cells/Berberine: 591; Scaffold/Cells: 304; Scaffold: 174; Berberine: 292; Control: 80. The combination treatment resulted in a nerve diameter over 7 times larger than the control and significantly larger than all other groups. 3. Axon Count: Scaffold/Cells/Berberine: 1224; Scaffold/Cells: 874; Scaffold: 204; Berberine: 371; Control: 37. The Scaffold/Cells/Berberine group had the highest number of regenerated axons, over 33 times more than the control. 4. Schwann Cell Count: Scaffold/Cells/Berberine: 1437; Scaffold/Cells: 1015; Scaffold: 107; Berberine: 391; Control: 58. The presence of cells and berberine significantly enhanced Schwann cell proliferation at the injury site. 5. New Nerve Formation (%): Scaffold/Cells/Berberine: 18.5%; Scaffold/Cells: 14.2%; Scaffold: 4.2%; Berberine: 6.1%; Control: 0.2%. The triple-combination therapy yielded the highest percentage of new nerve formation. 6. Blood Vessel Count: Scaffold/Cells/Berberine: 67; Scaffold/Cells: 49; Scaffold: 34; Berberine: 34; Control: 6. The Scaffold/Cells/Berberine group promoted the highest level of angiogenesis, which was over 11 times greater than the control.	No cytotoxicity of berberine on EnMSCs observed at concentrations up to 200 μM (cell viability >99%). Reduced inflammation observed in cell-treated groups. Good biocompatibility of the PAN/CS scaffold.	[70]

Table 2 Comprehensive Summary of in vitro Studies on Engineered CHM Delivery Systems for PN

Delivery Systems	Models	Effects[a]	References
Curcumin-loaded polycaprolactone nanofibers	PC12 cells	cellular uptake↑, neurite growth↑	[47]
LBP encapsulated in PLGA core-shell fibers	SCs, DRG neurons	SCs proliferation ↑, neurite length of DRG neurons↑	[48]
Curcumin and quercetin-loaded chitosan/hyaluronic acid nanoparticles	glioblastoma cells	glioblastoma cells death↑	[53]
NGF-loaded chitosan/hyaluronic acid nanoparticles	mouse DRG	nerve outgrowth↑	[53]
Aloe vera in solution and poly (3-Hydroxybutyrate-Co-3-Hydroxyvalerate) nanofibers	rat DRG acute axotomy	axonal outgrowth↑	[54]
LBP and NGF-loaded conductive nanofibrous	PC12 cells, DRG neurons	axon outgrowth↑	[56]
Chitosan/oxidized hydroxyethyl cellulose/reduced graphene oxide/ asiaticoside liposome-based hydrogel	PC12 cells, fibroblasts	PC12 cells differentiation and proliferation↑, The activity and collagen secretion of fibroblasts↓	[71]
Berberine-loaded nerve conduits contained with elatonin and graphene oxide-loaded hydrogels	RSC96 cells	RSC96 cells proliferation↑	[72]

Notes: [a] ↑ indicates promotion or upregulation; ↓ indicates inhibition or downregulation.

facilitate nutrient diffusion and SCs infiltration. Microenvironment correction occurs through two mechanisms: hesperidin-loaded hydrogels sustain 75.8% anti-inflammatory release over 14 days,[57] whereas curcumin systems scavenge 82.53% of DPPH radicals and shift macrophages toward anti-inflammatory M2 phenotypes via CD206 upregulation.[58]

Hydrogel-based delivery systems have demonstrated significant therapeutic advantages in both in vitro and in vivo studies, supported by their multi-targeted molecular actions. In vitro studies have shown that engineered hydrogels profoundly enhance nerve regeneration. Collagen hydrogels loaded with naringin double SCs proliferation compared to control surfaces, achieving an optical density value of 0.4 versus 0.2 after 72 hours of culture.[59] Conductive hydrogels incorporating reduced graphene oxide elevated neuronal differentiation to 77.96% in PC12 cells under electrical stimulation, leveraging electroactive properties to accelerate nerve maturation.[71] The regenerative benefits of these hydrogel systems are driven by their capacity to coordinately regulate multiple cellular processes. Key mechanisms include the promotion of Schwann cell proliferation and migration through ERK1/2 pathway activation and MMP-9 upregulation,[65] the suppression of apoptosis via caspase-3/9 downregulation,[65] and the enhancement of endogenous antioxidant defenses through Nrf2 pathway activation, elevating levels of SOD and GSH by 30% and 25%, respectively.[57,59,61] A central function is the effective polarization of macrophages from a pro-inflammatory M1 state to a regenerative M2 phenotype, evidenced by reductions in M1 markers of up to 50% and increases in M2 markers by as much as 2.5-fold.[58,60,63,64] Concurrently, these systems dampen neuroinflammation by inhibiting NF-κB signaling[60,64] and directly promote nerve repair by upregulating critical structural proteins such as MBP, βIII-tubulin, and GAP-43, thereby enhancing myelination and axonal extension.[57,59,60,63,65]

In animal models, functional and structural recovery is markedly superior to non-engineered interventions. Photoresponsive curcumin hydrogels triple myelinated axon density in sciatic nerve injuries, generating 360 fibers/μm² versus 104.67 fibers/μm² in crush-injury controls.[58] Functional restoration is equally striking: berberine-loaded alginate/chitosan hydrogels improve sciatic functional index (SFI) to −20.23 ± 1.35 after 8 weeks, dramatically surpassing untreated groups (−76.90 ± 4.12) and pure hydrogel controls (−46.00 ± 1.60).[64] Pain management capabilities are evidenced by curcumin nanocapsule hydrogels reducing thermal hyperalgesia and shortening paw withdrawal latency to 6 s compared to 12s in baseline models.[62] Chronic neuropathy interventions have shown sustained efficacy, with boronic ester-based hydrogels enhancing nerve conduction velocity to 25 m/s versus 10 m/s in constriction injury models.[61] Microenvironmental corrections underlie these outcomes. Curcumin systems shift macrophage polarization toward regenerative M2 phenotypes, elevating CD206 expression while suppressing pro-inflammatory cytokines.[58] Keratin-chitosan/curcumin hydrogels reduced muscle atrophy to 5.7% weight loss versus 40% weight loss in denervated controls, confirming the integrated tissue protection.[65] These multi-mechanistic effects collectively validate hydrogel carriers as potent platforms for nerve repair (Table 1 and Table 2).

Despite the compelling efficacy, four major challenges impede clinical adoption: dose optimization requires balancing efficacy and safety, as concentrations exceeding 1% naringin clog hydrogel pores[59] whereas 10% berberine induces cytotoxicity.[64] Degradation synchronization remains problematic, with alginate/chitosan hydrogels degrading too rapidly (80% mass loss in 14 days) for slow nerve regeneration,[57] whereas boronic ester hydrogels degrade only 20% over 28 days.[61] Manufacturing complexity hinders the scale-up of multifunctional systems such as liposome-hydrogel hybrids.[71] Technical dependencies on clinical-grade near-infrared/electrostimulation devices limit accessibility,[58,71] whereas long-term safety concerns persist regarding keratin immunogenicity[65] and metallic nanoparticle toxicity.[71]

The ability of hydrogels to correct microenvironmental imbalances and provide phase-adapted release, as demonstrated in these animal studies, positions them as a uniquely promising platform for PN treatment. Translating this microenvironment-modulating capacity into clinical benefit represents a central translational hypothesis moving forward.

Degradable Slow-Release Membranes

Within our therapeutic framework, degradable slow-release membranes emerge as a specialized platform for resolving the critical challenge of localized and sustained pharmacotherapy in PN. Engineered from biodegradable composites like chitosan-polyethylene oxide (PEO) and polylactic acid-glycolic acid-polyethylene glycol (PLGA-PEG), these membranes exhibit excellent biocompatibility and controlled degradation profiles. This design avoids severe immune responses while aligning with the extended timeline of nerve regeneration. For instance, chitosan-PEO membranes fabricated as thin films gradually degrade without inducing scar formation, providing a favorable microenvironment for axonal growth.[66] PLGA-PEG membranes, combining biodegradable PLGA with hydrophilic PEG, degrade over 85% in vitro within 10 weeks, matching the prolonged recovery process of nerve injuries, and their curved structure conforms to anatomical sites, such as the cavernous nerves, ensuring efficient localized drug delivery.[67]

The core function of these membranes lies in their ability to maintain stable, long-term drug release directly at the injury site. They enable sustained and dose-dependent release of curcumin: chitosan-PEO membranes maintain local curcumin concentrations to avoid systemic toxicity, while PLGA-PEG membranes achieve stable release (72.5–89.8% over 45 days) without burst effects, with higher curcumin ratios (1.4%) accelerating release to meet dynamic healing needs.[66,67] Additionally, their structural adaptability, such as trimable chitosan-PEO films for sciatic nerves and conformable PLGA-PEG membranes for cavernous nerves, facilitates their precise application. Multifunctional integration, such as chitosan's anti-fibrotic properties combined with curcumin's anti-inflammatory effects or PLGA-PEG's enhancement of curcumin solubility alongside nNOS upregulation, further improves therapeutic efficacy.[66,67]

Beyond their pharmacokinetic benefits, these membrane systems actively contribute to healing by mitigating bioavailability issues and correcting a dysregulated microenvironment. PLGA-PEG membranes maintain local curcumin concentrations for 45 days, whereas chitosan-PEO membranes reduce systemic clearance and enhance accumulation at injury sites.[66,67] These systems correct dysregulated microenvironments by scavenging reactive oxygen species (ROS), inhibiting pro-inflammatory cytokines, and reducing collagen I expression.[66,67]

In preclinical studies, engineered membranes have demonstrated superior efficacy compared to non-engineered membranes. For sciatic nerve transection in rats, chitosan-PEO + curcumin improves SFI (-64.9 ± 5.1 vs -75.3 ± 5.2 in the curcumin-only group) and increases myelinated fiber count (46.7 ± 7.4) and myelin thickness (2.19 ± 0.7 μm).[66] In cavernous nerve injury models, high-dose (1.4%) curcumin-loaded PLGA-PEG membranes improve erectile function (ICP/MAP: 0.68 ± 0.07) versus 0.51 ± 0.05 in the low-dose group and 0.34 ± 0.07 in the blank membrane group, while upregulating nNOS expression and reducing penile fibrosis[67] (Table 1).

Despite promising results, its clinical translation is challenging. Dose optimization is critical, as higher curcumin concentrations (1.4%) in PLGA-PEG membranes enhance efficacy but may increase local toxicity.[67] Membrane degradation rates must be synchronized with nerve regeneration; PLGA-PEG membranes degrade faster in vivo (~70% over 4 weeks) than in vitro, with the risk of premature loss of drug release.[67] Scalability and standardization of membrane fabrication, which ensures uniform drug loading and structural consistency, remain hurdles.[66] In addition, adapting the membrane to different types of nerve injuries (such as sciatic and cavernous nerves) needs to be validated in the human body to ensure clinical applicability.[67]

The localized and sustained pharmacotherapy achieved by degradable membranes in preclinical nerve injury models highlights their potential for focal neuropathies. The critical question of whether these release profiles and functional outcomes can be replicated in human nerves remains to be clinically investigated.

Functionalized Nerve Conduits

Within our therapeutic framework, functionalized nerve conduits constitute a definitive strategy for overcoming the challenge of structural repair in long-gap nerve defects. These conduits, crafted from polymers, such as chitosan, polyurethane (PU), polyacrylonitrile/chitosan (PAN/CS), and conductive composites, are engineered to align with the complexities of nerve repair. Chitosan-based conduits, for instance, feature tapered ends with differing inner diameters (0.8 mm at the thinner end and 1.8 mm at the thicker end), a design that addresses the size mismatch between proximal and distal nerves, which is an issue that plagues traditional uniform-diameter conduits. This allows tension-free suturing and reduces the risk of neuroma formation when bridging the proximal common peroneal nerve and distal mixed nerves (common peroneal and tibial).[68]

The functionality of these conduits is greatly enhanced by integrating drug delivery and active signaling capabilities. Gastrodin-modified PU conduits integrate biodegradability with sustained drug release: gastrodin is stabilized via covalent binding, avoiding rapid metabolism and maintaining local concentrations (with approximately 83.3% released over 18 days), while their conductivity (around 1.23×10^{-3} S/cm) supports electrical stimulation to boost nerve regeneration.[69] Other systems, like conductive L-ZBZPGM conduits incorporate graphene oxide for conductivity and feature interconnected pores (100–200 μm) that facilitate nutrient exchange, creating a favorable environment for SCs infiltration and axonal growth.[72] PAN/CS conduits, which combine the mechanical strength of synthetic PAN with the biocompatibility of chitosan, serve as dual carriers for berberine and stem cells, thereby enhancing cell adhesion and targeted drug delivery.[70]

These integrated systems produce their restorative effects through multi-mechanistic actions on the nerve regeneration process. Berberine inhibits TNF-α and iNOS,[72] gastrodin upregulates BDNF/GDNF to enhance myelination,[69] and chitosan conduits loaded with the modified formula Radix Hedysari (MFRH) stimulate the formation of myelinated fibers (approximately 46.7 fibers/μm²).[68] Functionally, chitosan/MFRH conduits improve the SFI (−64.9 versus −78.5 in controls) and nerve conduction velocity (approximately 35 m/s vs 20 m/s in controls).[68] PAN/CS conduits loaded with berberine and endometrial mesenchymal stem cells (EnMSCs) enhanced new nerve formation (18.5% vs 0.2% in controls) and reduced muscle atrophy, with denser and more organized myelinated fibers[70] (Table 1 and Table 2).

Despite promising preclinical results, its clinical translation has been hindered by several challenges. Optimization of the dose is crucial. Berberine at 200 μM slightly reduced EnMSC viability; therefore, precise adjustment is necessary, with 100 μM recognized as the optimal level.[70] Synchronizing degradation with nerve regeneration remains difficult; chitosan conduits degrade by approximately 80% within 16 weeks, whereas PAN/CS conduits degrade too slowly.[68,70] Additionally, conductive conduits rely on external electrical stimulation devices, which limits their use in resource-constrained settings.[69,72]

While functionalized conduits have demonstrated superior efficacy to autografts in specific rodent models of long-gap defects, these findings constitute a preclinical proof-of-concept. Whether they can become a definitive solution for human nerve injuries is a remarkable but unconfirmed hypothesis.

Challenges in Clinical Translation

Although engineered CHM delivery systems present a promising avenue for PN, several challenges impede their translation from laboratory research to clinical application. Understanding these challenges is crucial to develop feasible and effective engineering therapies for PN.

Material Biocompatibility and Long-Term Safety

The long-term biocompatibility of engineered materials is a foundational challenge that directly impacts the practical utility of all platforms in our therapeutic framework. Ongoing concerns exist regarding the chronic inflammation caused by nanocarriers and conduits.[75–77] Nanoparticles interacting with the immune system may provoke adverse immune

responses, as they can stimulate immune cells and lead to inflammation or severe immune reactions.[78] The potential immunogenicity of hydrogels requires comprehensive long-term human studies.[79] Additionally, complex multi-component systems, such as liposome-hydrogel hybrids or drug- and cell-integrated functionalized conduits, require thorough research beyond preliminary biocompatibility assessments. Furthermore, nanoparticles can accumulate in different organs, including the liver, spleen, and kidneys, causing organ-specific toxicity.[80] Consequently, the long-term effects of these materials remain unclear and require thorough preclinical toxicity assessment.

Precise Dosage Optimization and Controlled Release

Determining the optimal therapeutic dose within an engineered system is a complex challenge that sits at the heart of the spatiotemporal control principle.[81] A dosage that is effective during the inflammatory phase may be insufficient or even counterproductive in the regenerative phase, highlighting the need for phase-specific dosing strategies. Although high concentrations of active compounds may enhance efficacy, they can also induce cytotoxicity, disrupt the delivery system framework, and cause local toxicity.[82,83] Conversely, insufficient dosing failed to achieve the therapeutic threshold.[84] Aligning the degradation rate of the carrier material with the nerve repair timeline is equally challenging, but vital for sustained, phase-appropriate drug release. Predictable and linear release profiles are still hard to achieve.

Targeting Specificity and Overcoming Biological Barriers

The challenge of targeting specificity directly determines whether the strategic positioning of nanocarriers in our framework is feasible. Although ligand-mediated strategies are promising for improving targeted delivery, further refinement is required to ensure precision and minimize off-target accumulation and systemic toxicity. This imperfect targeting undermines the core advantage of nanocarriers—their ability to provide high local drug concentrations at the nerve injury site while minimizing side effects. The effectiveness of these systems in crossing the BNB complex in human PN needs rigorous validation in more clinically relevant models to confirm their role as a primary solution for BNB impermeability. The effectiveness of these systems in crossing the BNB complex in human PN needs rigorous validation in more clinically relevant models to confirm whether they can serve as the primary solution for BNB impermeability.

Integration with Clinical Procedures and Accessibility

The dependency of many advanced systems on external stimuli creates a significant gap between their theoretical potential within our framework and their practical clinical utility.[85,86] Conductive scaffolds and conduits require integration with clinical-grade electrical stimulation devices, which may not be readily available or practical in a clinical setting.[87] Similarly, photoresponsive systems rely on specific NIR light sources for controlled drug release.[88,89] The technical complexity and costs associated with these dependencies limit their clinical accessibility, particularly in areas with limited resources.

Scalability, Manufacturing Consistency, and Quality Control

Reproducible and scalable manufacturing is a translational precondition that determines whether the precise design features central to our framework can be reliably replicated. This process requires reliable acquisition of precise design parameters, which are crucial for therapeutic efficacy. But when transitioning from bench-scale synthesis to industrial production under Good Manufacturing Practice (GMP) standards, achieving this becomes even more challenging. A primary obstacle lies in the inherent variability of precision manufacturing techniques. Critical processes such as coaxial electrospinning for core-shell fibers and microfluidics for nanocarrier synthesis are easily affected by batch-to-batch inconsistencies. These variations are reflected in key physical attributes, including fiber diameter and nanoparticle size distribution, ultimately compromising the uniformity of drug loading and release kinetics and leading to unpredictable biological effects.[90–92] Scaling these processes while maintaining strict control over these critical quality attributes represents a significant engineering hurdle. Beyond process control, the consistent sourcing of biomedical-grade natural and synthetic polymers is fundamental. Moreover, industrial-scale processing may degrade the sensitive bioactive compounds in CHM, as their complex chemical profiles can be altered by factors such as shear stress, exposure to

solvents, or elevated temperatures encountered during manufacturing.[93–95] Finally, establishing robust and validated analytical methods is crucial. The successful transition to industrial production requires the adoption of a "Quality by Design" framework. This approach not only requires in-process monitoring and control of the carrier's physical properties, but also the chemical consistency and quality of the encapsulated CHM actives, which can be compromised by physicochemical interactions within the formulation[96,97] and processing variables.[98] The comprehensive standardization of these complex manufacturing processes to meet GMP standards constitutes a major obstacle, directly affecting product safety, efficacy, and ultimate clinical success.

Regulatory Pathways and Standardization

The clinical translation of engineered CHM delivery systems is further complicated by their status as combination products, integrating device, drug, and sometimes biological components, which places them within a complex and evolving regulatory landscape. A foundational challenge is their classification by major regulatory agencies such as the FDA and European Medicines Agency (EMA). A pivotal first step involves determining the product's Primary Mode of Action (PMOA)—that is, whether the principal therapeutic action is attributable to the physical scaffold or the encapsulated herbal active ingredient. This classification dictates the lead regulatory center and the specific set of guidelines for approval, a decision that is often ambiguous for novel platforms where the scaffold itself exerts bioactive effects.[99,100] This classification challenge is compounded by a lack of standardized preclinical testing protocols. There is a pressing need for harmonized methods to evaluate long-term biodegradation, chronic toxicity of degradation byproducts, and biodistribution.[99,101,102] The multicomponent nature of CHM formulations introduces additional complexity, requiring novel regulatory science approaches to ensure consistent quality, safety, and efficacy, particularly concerning potential physicochemical interactions and synergistic effects.[96,97] Consequently, the Chemistry, Manufacturing, and Controls (CMC) documentation required for a regulatory submission is exceptionally demanding. It must provide a comprehensive and validated account of the entire manufacturing process, define all critical quality attributes, and demonstrate product stability.[99,100] Therefore, generating necessary long-term safety and batch to bioequivalence data for these complex products is a resource intensive and time-consuming task, posing significant barriers to their market access.

Bridging the Preclinical-Clinical Gap

Translating the success from rodent models to humans remains the ultimate validation hurdle for the entire proposed framework. It is important to verify the effectiveness and safety of these delivery systems in large animal models that can better replicate human nerve anatomy, regeneration rate, and disease pathophysiology; however, resources are often insufficient.[100,102] Moreover, proving that there is a significant improvement in functional recovery compared to current clinical standards, considerable time, and investment are required. A delivery system designed for specific types of nerves, such as the sciatic nerve conduit and sponge-like nerve membrane, must be carefully clinically validated to adapt to the different anatomical and pathological environments encountered in human PN.

Clinical Evidence and Gaps

Current Clinical Status: A Preclinical Landscape

A systematic search of international and domestic clinical trial registries (including ClinicalTrials.gov and the Chinese Clinical Trial Registry) confirms that, to date, no clinical trials have been initiated to evaluate the engineered CHM delivery systems discussed in this review for the treatment of peripheral neuropathy in humans. While clinical trials exist for oral CHM extracts and for synthetic drug-loaded advanced delivery systems, the specific combination of CHM bioactives with engineered carriers (nanocarriers, hydrogels, membranes, conduits) remains an unknown field in clinical research. The convincing therapeutic outcomes detailed throughout this review are entirely derived from preclinical models. Consequently, all assertions regarding the efficacy, optimal design parameters, and mechanisms of action of these systems must be anchored in their preclinical nature. The conclusions drawn serve to generate hypotheses for their

future clinical application rather than to confirm their therapeutic value in humans. This clearly highlights a significant and critical translational gap.

Mapping the Minimal Clinical Package

Translating promising preclinical findings into clinical application requires a clear, step-by-step development pathway. Making this transition depends on generating a core set of evidence that addresses the special challenges of these combination products. The first and most crucial step is to conduct in-depth safety evaluations according to GLP standards. These studies, ideally performed in two different species, must go beyond standard toxicity screening to specifically investigate the long-term fate of the delivery systems. Critical questions that need answers include: whether the implantation site might cause long-term local inflammation, the specific patterns of nanocarrier accumulation and clearance rates in organs, and the safety of the materials themselves and their breakdown products for the nervous system.

At the same time, it is essential to fully understand how these systems behave in the body, namely their pharmacokinetics and distribution, in large animal models relevant to human medicine. Data from rodent studies, although valuable, are not sufficient to predict how these systems will perform in humans. Research must precisely measure how efficiently they cross the BNB, confirm whether the targeted delivery claimed for functionalized nanocarriers truly reduces accumulation in non-target organs, and clarify the full metabolic pathways of these complex systems. This stage is vital for reducing the risks of human trials, as it checks whether the basic pharmacological principles observed in small animals still hold true in a physiological environment more similar to ours.

The design of the first human trials should be guided by a careful, step-by-step approach to managing risks. A prudent strategy for a First-in-Human study would focus on a clearly defined group of patients where the delivery system can be applied directly to a specific area. An example would be during surgery to repair a localized nerve injury. This method confines the treatment to a precise location, greatly reduces exposure to the rest of the body, and makes it easier to evaluate how well the local area tolerates the implant. The main goal of such a Phase I study would be to build a complete safety profile, while measurements of functional recovery could serve as initial indicators to look for signs of effectiveness. By outlining this route, which encompasses rigorous safety and distribution studies in large animals and a carefully planned initial clinical investigation, the field can build a solid bridge connecting the current state of preclinical research to future therapeutic application.

Future Perspectives

The development of engineered traditional CHM delivery systems has brought great hope for PN treatment. To bridge the gap between preclinical promise and clinical reality, future efforts must be strategically guided by the framework proposed in this review, focusing on enhancing the intelligence, scalability, and personalization of these platforms.

We hypothesize that the next generation of CHM delivery systems should evolve towards intelligent multifunctionality to fully realize the spatiotemporal control principle of our framework. By combining stimulus response mechanisms such as enzyme-, redox-, or biomarker-triggered release with real-time biosensing, it is possible to autonomously adapt to dynamic nerve injury microenvironments.[103–106] For instance, systems that detect elevated TNF-α or ROS levels to precisely release anti-inflammatory agents or neurotrophic factors during the inflammatory or regenerative phases would overcome current limitations in spatiotemporal control. By combining CHM with advanced models, such as gene therapy or immune modulators, multiple pathological pathways can be synergistically targeted to enhance regeneration outcomes and address heterogeneity issues.[42,107–110]

Scalable production and rigorous validation of long-term safety are crucial for clinical implementation. Scalable and repeatable production requires advanced technologies, such as continuous flow microfluidics for nanocarriers and automated 3D bioprinting for hydrogels/conduits.[111–113] This ensured consistency in drug loading, structural characteristics (such as pore size and fiber diameter), and degradation rates across different batches.[114] Long-term biocompatibility must be rigorously validated through large-scale animal studies, such as primate models, with a focus on the chronic toxicity analysis of degradation byproducts and immunogenicity.[115–117] There is an urgent need for standardized

regulatory frameworks for combination products, including devices, drugs, and biologics, along with harmonized protocols for assessing biodistribution, bioaccumulation, and immunotoxicity.

Personalization is proposed as a critical frontier for optimizing therapeutic efficacy and safety in future clinical translation.[118,119] Using clinical imaging data, 3D-printed conduits and hydrogels can be customized to match the anatomical structure of nerve defects and support individualized CHM dosing.[120–122] Combining machine learning with multi-omics data shows potential for predicting optimal CHM combinations and doses, mitigating physicochemical incompatibilities and cytotoxicity risks.[123,124]

Improving accessibility and clinical practicality are crucial for its widespread adoption. By creating self-powered systems and reducing the dependence on external stimuli, such as clinical-grade near-infrared devices and electrical stimulators, their usefulness will greatly increase, particularly in environments with limited resources.[125,126] Cost-effective solutions, such as optimizing CHM extraction efficiency or utilizing biosynthetic analogs of rare herbal compounds, could enhance affordability.[127,128] Ultimately, successful translation depends on sustained interdisciplinary collaboration among material scientists, neural engineers, herbal pharmacologists, clinicians, and regulatory experts.

Limitations

As a narrative review, this work has certain inherent limitations. The selection of literature, while aimed at representing key advances and illustrating the proposed framework, was not based on a systematic, reproducible search of all databases. Consequently, it may be subject to selection bias, and some relevant studies might have been overlooked. Furthermore, narrative reviews do not typically include a formal risk-of-bias assessment of the included preclinical studies, which is a standard component of systematic reviews. Therefore, the findings and conclusions presented here should be interpreted as a critical narrative synthesis and a proposal for a new perspective, intended to guide and inspire future research, rather than as an exhaustive or quantitatively definitive summary of the evidence.

Conclusions

Preclinical evidence positions engineered CHM delivery systems as a potentially transformative approach to overcoming the multifaceted therapeutic challenges of PN. This review has not only organized these advances but also established a conceptual framework. It systematically links the core pathological challenges of PN—including pathological heterogeneity, spatiotemporal dynamics, BNB impermeability, microenvironmental imbalance, and structural defects—to the functional capabilities of specific delivery platforms. Through this perspective, we have organized a clear taxonomy: nanocarriers are the primary solution for BNB penetration and targeted, stimuli-responsive delivery; hydrogels excel at modulating the microenvironment and providing sustained, phase-adapted release; degradable membranes offer localized and prolonged pharmacotherapy for focal injuries; and functionalized nerve conduits are indispensable for bridging long-gap structural defects.

By addressing the inherent limitations of CHM, these engineered platforms have unlocked its multifactorial therapeutic potential, demonstrating significant preclinical efficacy in enhancing nerve regeneration and functional recovery. However, significant translational hurdles remain to be overcome. Key challenges include ensuring the long-term biocompatibility of materials, maintaining consistent scalable manufacturing, and optimizing the dosage to balance efficacy with cytotoxicity. Dependence on external triggers restricts accessibility and the absence of standardized regulatory frameworks makes clinical adoption more complex. Crucially, successful translation requires validation in large animal models that replicate human neuroanatomy and disease progression, which demands interdisciplinary collaboration and substantial investment.

In the future, combining smart multifunctionality, personalized design, and affordable production will be important. Collaboration among material scientists, clinicians, herbal pharmacologists, and regulatory authorities is crucial to move these systems from preclinical to clinical applications. If these challenges are resolved, engineered CHM delivery can redefine PN management, shift from palliative care to restorative therapy, and establish a new standard for precision neuromedicine.

In summary, this review synthesizes a compelling preclinical data for engineered CHM delivery systems. The framework and conclusions presented herein are primarily hypothesis-generating, outlining a roadmap for future research that must now be validated through rigorous clinical investigation.

Abbreviations

PN, Peripheral neuropathy; BNB, Blood-nerve barrier; CHM, Chinese herbal medicine; DPN, Diabetic peripheral neuropathy; BBB, Blood-brain barrier; NGCs, Nerve guiding catheters; LBP, Lycium barbarum polysaccharides; GBE, Ginkgo biloba extract; PLGA, Poly (lactic-co-glycolic acid); ADSCs, Adipose-derived stem cells; DRG, Dorsal root ganglia; CMT, Charcot-Marie-Tooth; SCs, Schwann cells; SFI, sciatic functional index; PEO, Chitosan-polyethylene oxide; PLGA-PEG, Polylactic acid-glycolic acid-polyethylene glycol; ROS, Reactive oxygen species; PU, Polyurethane; PAN/CS, Polyacrylonitrile/chitosan; MFRH, Modified formula Radix Hedysari; EnMSCs, Endometrial mesenchymal stem cells; GMP, Good Manufacturing Practice; FDA, The US Food and Drug Administration; EMA, The European Medicines Agency.

Funding

This work was supported by the National Natural Science Foundation of China (82301567), the China Postdoctoral Science Foundation (2024M761195), and the General Project of Jiangsu Provincial Health Commission (H2023112).

Disclosure

The authors declare that there is no conflict of interest in this work.

References

1. Chiaramonte R, Pavone V, Testa G, et al. The role of physical exercise and rehabilitative implications in the process of nerve repair in peripheral neuropathies: a systematic review. *Diagnostics*. 2023;13:3.
2. Song Q, Sun M, Lewis K, Choi JH, Manor B, Li L. Hoffmann reflex measured from lateral gastrocnemius is more reliable than from soleus among elderly with peripheral neuropathy. *Front Aging Neurosci*. 2022;14:800698. doi:10.3389/fnagi.2022.800698
3. Matthews TP, Zhang C, Yao DK, Maslov K, Wang LV. Label-free photoacoustic microscopy of peripheral nerves. *J Biomed Opt*. 2014;19 (1):16004. doi:10.1117/1.JBO.19.1.016004
4. Sun X, Zhu Y, Yin HY, et al. Differentiation of adipose-derived stem cells into Schwann cell-like cells through intermittent induction: potential advantage of cellular transient memory function. *Stem Cell Res Ther*. 2018;9(1):133. doi:10.1186/s13287-018-0884-3
5. Jo HG, Baek E, Lee D. Comparative efficacy of east asian herbal formulae containing astragali radix-Cinnamomi Ramulus Herb-Pair against diabetic peripheral neuropathy and mechanism prediction: a Bayesian network meta-analysis integrated with network pharmacology. *Pharmaceutics*. 2023;15(5):1361. doi:10.3390/pharmaceutics15051361
6. Yilmaz S, Gur C, Kucukler S, Akaras N, Kandemir FM. Zingerone attenuates sciatic nerve damage caused by sodium arsenite by inhibiting NF-kappaB, caspase-3, and ATF-6/CHOP pathways and activating the Akt2/FOXO1 pathway. *Iran J Basic Med Sci*. 2024;27(4):485–491. doi:10.22038/IJBMS.2023.74088.16094
7. Acaster S, Lo SH, Nestler-Parr S. A survey exploring caregiver burden and health-related quality of life in hereditary transthyretin amyloidosis. *Orphanet J Rare Dis*. 2023;18(1):17. doi:10.1186/s13023-022-02601-5
8. Talaei SA, Banafshe HR, Moravveji A, Shabani M, Tehrani SS, Abed A. Anti-nociceptive effect of black seed oil on an animal model of chronic constriction injury. *Res Pharm Sci*. 2022;17(4):383–391. doi:10.4103/1735-5362.350239
9. Razzaq A, Hussain G, Rasul A, et al. seed preparation promotes functional recovery and attenuates oxidative stress in a mouse model of sciatic nerve crush injury. *BMC Complement Med Ther*. 2020;20(1):181. doi:10.1186/s12906-020-02950-3
10. Shahid W, Kumar R, Shaikh A, Kumar S, Jameel R, Fareed S. Comparison of the efficacy of duloxetine and pregabalin in pain relief associated with diabetic neuropathy. *Cureus*. 2019;11(7):e5293. doi:10.7759/cureus.5293
11. Sugimoto M, Takagi T, Suzuki R, et al. Drug treatment for chemotherapy-induced peripheral neuropathy in patients with pancreatic cancer. *Fukushima J Med Sci*. 2022;68(1):1–10. doi:10.5387/fms.2021-32
12. Dawson ET, Hocker SE. Neurologic complications of commonly used drugs in the hospital setting. *Curr Neurol Neurosci Rep*. 2016;16(4):35. doi:10.1007/s11910-016-0636-7
13. Little JW, Ford A, Symons-Liguori AM, et al. Endogenous adenosine A3 receptor activation selectively alleviates persistent pain states. *Brain*. 2015;138(Pt 1):28–35. doi:10.1093/brain/awu330
14. Anand P, Elsafa E, Privitera R, et al. Rational treatment of chemotherapy-induced peripheral neuropathy with capsaicin 8% patch: from pain relief towards disease modification. *J Pain Res*. 2019;12:2039–2052. doi:10.2147/JPR.S213912
15. Uberall M, Bosl I, Hollanders E, Sabatschus I, Eerdekens M. Painful diabetic peripheral neuropathy: real-world comparison between topical treatment with lidocaine 700 mg medicated plaster and oral treatments. *BMJ Open Diabetes Res Care*. 2022;10(6):e003062. doi:10.1136/bmjdrc-2022-003062
16. Chkheidze R, Pytel P. What every neuropathologist needs to know: peripheral nerve biopsy. *J Neuropathol Exp Neurol*. 2020;79(4):355–364. doi:10.1093/jnen/nlaa012

17. Dubovy P. Wallerian degeneration and peripheral nerve conditions for both axonal regeneration and neuropathic pain induction. *Ann Anat*. 2011;193(4):267–275. doi:10.1016/j.aanat.2011.02.011
18. Pallas WD, Pak ES, Hannan JL. In vitro high glucose increases apoptosis, decreases nerve outgrowth, and promotes survival of sympathetic pelvic neurons. *Sex Med*. 2023;11(1):qfac009. doi:10.1093/sexmed/qfac009
19. Liang J, Zhang N, Li G, et al. Piezo1 promotes peripheral nerve fibrotic scar formation through Schwann cell senescence. *Neurosci Lett*. 2024;837:137916. doi:10.1016/j.neulet.2024.137916
20. Paris A, Bora P, Parolo S, et al. An age-dependent mathematical model of neurofilament trafficking in healthy conditions. *CPT Pharmacometrics Syst Pharmacol*. 2022;11(4):447–457. doi:10.1002/psp4.12770
21. Magge RS, DeAngelis LM. The double-edged sword: neurotoxicity of chemotherapy. *Blood Rev*. 2015;29(2):93–100. doi:10.1016/j.blre.2014.09.012
22. Rochford AE, Carnicer-Lombarte A, Curto VF, Malliaras GG, Barone DG. When bio meets technology: biohybrid neural interfaces. *Adv Mater*. 2020;32(15):e1903182. doi:10.1002/adma.201903182
23. Gaudin R, Knipfer C, Henningsen A, Smeets R, Heiland M, Hadlock T. Approaches to peripheral nerve repair: generations of biomaterial conduits yielding to replacing autologous nerve grafts in Craniomaxillofacial surgery. *Biomed Res Int*. 2016;2016:3856262. doi:10.1155/2016/3856262
24. Saikia B, Buragohain L, Barua CC, et al. Evaluation of anti-amnesic effect of Conyza bonariensis in rats. *Indian J Pharmacol*. 2022;54(2):102–109. doi:10.4103/ijp.ijp_201_19
25. Chen YQ, Zhang YX, Zhang X, et al. Mechanism and application of Chinese herb medicine in treatment of peripheral nerve injury. *Chin J Integr Med*. 2025;31(3):270–280. doi:10.1007/s11655-024-4004-1
26. Yang S, Hao S, Wang Q, Lou Y, Jia L, Chen D. The interactions between traditional Chinese medicine and gut microbiota: global research status and trends. *Front Cell Infect Microbiol*. 2022;12:1005730. doi:10.3389/fcimb.2022.1005730
27. Wang YY, Li J, Wu ZR, et al. Insights into the molecular mechanisms of Polygonum multiflorum Thunb-induced liver injury: a computational systems toxicology approach. *Acta Pharmacol Sin*. 2017;38(5):719–732. doi:10.1038/aps.2016.147
28. Viezuina DM, Musa I, Aldea M, et al. Gelatin-based hydrogels for peripheral nerve regeneration: a multifunctional vehicle for cellular, molecular, and pharmacological therapy. *Gels*. 2025;11(7):490. doi:10.3390/gels11070490
29. Kim JH, Ha WR, Park JH, et al. Influence of herbal combinations on the extraction efficiencies of chemical compounds from Cinnamomum cassia, Paeonia lactiflora, and Glycyrrhiza uralensis, the herbal components of Gyeji-tang, evaluated by HPLC method. *J Pharm Biomed Anal*. 2016;129:50–59. doi:10.1016/j.jpba.2016.06.044
30. Shibuya K, Misawa S, Nasu S, et al. Safety and efficacy of intravenous ultra-high dose methylcobalamin treatment for peripheral neuropathy: a phase I/II open label clinical trial. *Intern Med*. 2014;53(17):1927–1931. doi:10.2169/internalmedicine.53.1951
31. Buttner R, Schulz A, Reuter M, et al. Inflammaging impairs peripheral nerve maintenance and regeneration. *Aging Cell*. 2018;17(6):e12833. doi:10.1111/acel.12833
32. Mori I. Highlighting the 'blood-nerve barrier' in virology research. *Acta Virol*. 2018;62(1):28–32. doi:10.4149/av_2018_103
33. Stubbs EB. Targeting the blood-nerve barrier for the management of immune-mediated peripheral neuropathies. *Exp Neurol*. 2020;331:113385. doi:10.1016/j.expneurol.2020.113385
34. Shimizu F, Sano Y, Maeda T, et al. Peripheral nerve pericytes originating from the blood-nerve barrier expresses tight junctional molecules and transporters as barrier-forming cells. *J Cell Physiol*. 2008;217(2):388–399. doi:10.1002/jcp.21508
35. Sharma C, Kaur I, Singh H, Grover IS, Singh J. A randomized comparative study of methylcobalamin, methylcobalamin plus pregabalin and methylcobalamin plus duloxetine in patients of painful diabetic neuropathy. *Indian J Pharmacol*. 2021;53(5):358–363. doi:10.4103/ijp.ijp_1159_20
36. Asconape JJ. Use of antiepileptic drugs in hepatic and renal disease. *Handb Clin Neurol*. 2014;119:417–432.
37. Dawi J, Tumanyan K, Tomas K, et al. Diabetic foot ulcers: pathophysiology, immune dysregulation, and emerging therapeutic strategies. *Biomedicines*. 2025;13(5):1076. doi:10.3390/biomedicines13051076
38. Llorian-Salvador M, Cabeza-Fernandez S, Gomez-Sanchez JA, de la Fuente AG. Glial cell alterations in diabetes-induced neurodegeneration. *Cell Mol Life Sci*. 2024;81(1):47. doi:10.1007/s00018-023-05024-y
39. Alizadeh SD, Jahani S, Rukerd MRZ, et al. Human studies of the efficacy and safety of stem cells in the treatment of diabetic peripheral neuropathy: a systematic review and meta-analysis. *Stem Cell Res Ther*. 2024;15(1):442. doi:10.1186/s13287-024-04033-3
40. Tesfaye S, Wilhelm S, Lledo A, et al. Duloxetine and pregabalin: high-dose monotherapy or their combination? The "COMBO-DN study"–a multinational, randomized, double-blind, parallel-group study in patients with diabetic peripheral neuropathic pain. *Pain*. 2013;154(12):2616–2625. doi:10.1016/j.pain.2013.05.043
41. Tabatabai TS, Alizadeh M, Farahani MK, Ehterami A, Kloucheh SG, Salehi M. Peripheral nerve repair: historical perspectives, current advances, and future directions in natural and synthetic neural conduits. *J Neurosci Res*. 2025;103(7):e70060. doi:10.1002/jnr.70060
42. Liu K, Yan L, Li R, et al. 3D printed personalized nerve guide conduits for precision repair of peripheral nerve defects. *Adv Sci*. 2022;9(12):e2103875. doi:10.1002/advs.202103875
43. Yu XY, Lin SG, Zhou ZW, et al. Role of P-glycoprotein in the intestinal absorption of tanshinone IIA, a major active ingredient in the root of Salvia miltiorrhiza Bunge. *Curr Drug Metab*. 2007;8(4):325–340. doi:10.2174/138920007780655450
44. Estolano-Cobian A, Alonso MM, Diaz-Rubio L, Ponce CN, Cordova-Guerrero I, Marrero JG. Tanshinones and their derivatives: heterocyclic ring-fused diterpenes of biological interest. *Mini Rev Med Chem*. 2021;21(2):171–185. doi:10.2174/1389557520666200429103225
45. Gu Q, Xiao W, Zhu Y, et al. Microfluidic approach for enhanced paeoniflorin transdermal delivery: a comparative study on different chips and mixing dynamics. *AAPS Pharm Sci Tech*. 2025;26(1):39. doi:10.1208/s12249-024-03033-z
46. Zhang J, Qi H, Wang M, Wei Y, Liang H. Enzymatically hydrolyzed sodium caseinate nanoparticles efficiently enhancing the solubility, stability, and antioxidant and anti-biofilm activities of hydrophobic Tanshinone IIA. *J Mater Chem B*. 2023;11(11):2440–2454. doi:10.1039/D2TB02263J
47. Shrestha S, Jang SR, Shrestha BK, Park CH, Kim CS. Engineering 2D approaches fibrous platform incorporating turmeric and polyaniline nanoparticles to predict the expression of betaIII-Tubulin and TREK-1 through qRT-PCR to detect neuronal differentiation of PC12 cells. *Mater Sci Eng C Mater Biol Appl*. 2021;127:112176. doi:10.1016/j.msec.2021.112176

48. Wang J, Tian L, He L, et al. Lycium barbarum polysaccharide encapsulated Poly lactic-co-glycolic acid Nanofibers: cost effective herbal medicine for potential application in peripheral nerve tissue engineering. *Sci Rep*. 2018;8(1):8669. doi:10.1038/s41598-018-26837-z
49. Gong H, Chen Z. Adipose-derived stem cells and ginkgo biloba extract-loaded PCL/gelatin nanofibrous scaffolds for peripheral nerve injury repair: the impact of physical activity. *Acta Bioeng Biomech*. 2023;25(4):35–47. doi:10.37190/abb-02323-2023-06
50. Dwivedi S, Gottipati A, Ganugula R, et al. Oral nanocurcumin alone or in combination with insulin alleviates STZ-induced diabetic neuropathy in rats. *Mol Pharm*. 2022;19(12):4612–4624. doi:10.1021/acs.molpharmaceut.2c00465
51. Zhao S, Yang J, Han X, et al. Effects of nanoparticle-encapsulated curcumin on HIV-gp120-associated neuropathic pain induced by the P2X(3) receptor in dorsal root ganglia. *Brain Res Bull*. 2017;135:53–61. doi:10.1016/j.brainresbull.2017.09.011
52. Jia T, Rao J, Zou L, et al. Nanoparticle-encapsulated curcumin inhibits diabetic neuropathic pain involving the P2Y12 Receptor in the Dorsal Root Ganglia. *Front Neurosci*. 2017;11:755. doi:10.3389/fnins.2017.00755
53. Sabourian P, Ji J, Lotocki V, et al. Facile design of autogenous stimuli-responsive chitosan/hyaluronic acid nanoparticles for efficient small molecules to protein delivery. *J Mater Chem B*. 2020;8(32):7275–7287. doi:10.1039/D0TB00772B
54. Romero-Aleman MD, Perez-Galvan JM, Hernandez-Rodriguez JE, Monzon-Mayor M. The potential of aloe vera in solution and in blended nanofibers containing poly (3-hydroxybutyrate-Co-3-Hydroxyvalerate) as substrates for neurite outgrowth. *J Biomed Mater Res A*. 2025;113(1): e37825. doi:10.1002/jbm.a.37825
55. Caillaud M, Msheik Z, Ndong-Ntoutoume GM, et al. Curcumin-cyclodextrin/cellulose nanocrystals improve the phenotype of Charcot-Marie-Tooth-1A transgenic rats through the reduction of oxidative stress. *Free Radic Biol Med*. 2020;161:246–262. doi:10.1016/j.freeradbiomed.2020.09.019
56. Wang J, Liu Y, Lv M, et al. Regulation of nerve cells using conductive nanofibrous scaffolds for controlled release of Lycium barbarum polysaccharides and nerve growth factor. *Regen Biomater*. 2023;10:rbad038. doi:10.1093/rb/rbad038
57. Bagher Z, Ehterami A, Nasrolahi M, Azimi M, Salehi M. Hesperidin promotes peripheral nerve regeneration based on tissue engineering strategy using alginate/chitosan hydrogel: in vitro and in vivo study. *Int J Polym Mater Polym Biomater*. 2020;70(5):299–308. doi:10.1080/00914037.2020.1713781
58. Bi S, He C, Zhou Y, et al. Versatile conductive hydrogel orchestrating neuro-immune microenvironment for rapid diabetic wound healing through peripheral nerve regeneration. *Biomaterials*. 2025;314:122841. doi:10.1016/j.biomaterials.2024.122841
59. Samadian H, Vaez A, Ehterami A, et al. Sciatic nerve regeneration by using collagen type I hydrogel containing naringin. *J Mater Sci Mater Med*. 2019;30(9):107. doi:10.1007/s10856-019-6309-8
60. Zeng R, Xiong Y, Lin Z, et al. Novel cocktail therapy based on multifunctional supramolecular hydrogel targeting immune-angiogenesis-nerve network for enhanced diabetic wound healing. *J Nanobiotechnology*. 2024;22(1):749. doi:10.1186/s12951-024-03038-7
61. Kong Y, Shi W, Zheng L, et al. Corrigendum to "In situ delivery of a curcumin-loaded dynamic hydrogel for the treatment of chronic peripheral neuropathy" [Journal of Controlled Release, 357 (2023) 319-332]. *J Control Release*. 2024;371(371):621. doi:10.1016/j.jconrel.2024.03.012
62. Jiang X, Wang S, Chen H. A novel fabrication of dose-dependent injectable curcumin biocomposite hydrogel system anesthetic delivery method for care and management of musculoskeletal pain. *Dose Response*. 2020;18(3):1559325820929555. doi:10.1177/1559325820929555
63. Ebrahimi MH, Samadian H, Davani ST, et al. Peripheral nerve regeneration in rats by chitosan/alginate hydrogel composited with Berberine and Naringin nanoparticles: in vitro and in vivo study. *J Mol Liq*. 2020;318.
64. Rahmati M, Ehterami A, Saberani R, et al. Improving sciatic nerve regeneration by using alginate/chitosan hydrogel containing berberine. *Drug Deliv Transl Res*. 2021;11(5):1983–1993. doi:10.1007/s13346-020-00860-y
65. Sun X, Huang X, Liang Q, et al. Curcumin-loaded keratin-chitosan hydrogels for enhanced peripheral nerve regeneration. *Int J Biol Macromol*. 2024;272(Pt 2):132448. doi:10.1016/j.ijbiomac.2024.132448
66. Moattari M, Moattari F, Kouchesfahani HM, et al. Curcumin and biodegradable membrane promote nerve regeneration and functional recovery after sciatic nerve transection in adult rats. *Ann Plast Surg*. 2018;81(3):335–339. doi:10.1097/SAP.0000000000001566
67. Yang L, Ren Z, Liu Z, et al. Curcumin slow-release membrane promotes erectile function and penile rehabilitation in a rat model of cavernous nerve injury. *J Tissue Eng Regen Med*. 2022;16(9):836–849. doi:10.1002/term.3334
68. Zhang F, Li Q, Ma B, Zhang M, Kou Y. Chitosan-based conduits with different inner diameters at both ends combined with modified formula radix hedysari promote nerve transposition repair. *Front Biosci*. 2023;28(11):298. doi:10.31083/j.fbl2811298
69. Yang H, Li Q, Li L, et al. Gastrodin modified polyurethane conduit promotes nerve repair via optimizing Schwann cells function. *Bioact Mater*. 2022;8:355–367. doi:10.1016/j.bioactmat.2021.06.020
70. Bostani A, Hoveizi E, Naddaf H, Razeghi J. Nerve regeneration through differentiation of endometrial-derived mesenchymal stem cells into nerve-like cells using polyacrylonitrile/chitosan conduit and berberine in a rat sciatic nerve injury model. *Mol Neurobiol*. 2025;62(2):1493–1510. doi:10.1007/s12035-024-04344-9
71. Zheng F, Li R, He Q, et al. The electrostimulation and scar inhibition effect of chitosan/oxidized hydroxyethyl cellulose/reduced graphene oxide/asiaticoside liposome based hydrogel on peripheral nerve regeneration in vitro. *Mater Sci Eng C Mater Biol Appl*. 2020;109:110560. doi:10.1016/j.msec.2019.110560
72. Xu R, He H, Deng H, et al. Study of conductive nerve conduits for anti-inflammatory and antioxidant effects. *RSC Adv*. 2025;15(18):14136–14151. doi:10.1039/D5RA00997A
73. Jahromi HK, Farzin A, Hasanzadeh E, et al. Enhanced sciatic nerve regeneration by poly-L-lactic acid/multi-wall carbon nanotube neural guidance conduit containing Schwann cells and curcumin encapsulated chitosan nanoparticles in rat. *Mater Sci Eng C Mater Biol Appl*. 2020;109:110564. doi:10.1016/j.msec.2019.110564
74. Ge X, Wu S, Shen W, et al. Preparation of polyvinylidene fluoride-gold nanoparticles electrospinning nanofiber membranes. *Bioengineering*. 2022;9(4). doi:10.3390/bioengineering9040130
75. Svadlakova T, Hubatka F, Turanek Knotigova P, et al. Proinflammatory effect of carbon-based nanomaterials vitro study on stimulation of inflammasome nlrp3 via destabilisation of lysosomes. *Nanomaterials*. 2020;10:3.
76. Wei X, Shao B, He Z, et al. Cationic nanocarriers induce cell necrosis through impairment of Na(+)/K(+)-ATPase and cause subsequent inflammatory response. *Cell Res*. 2015;25(2):237–253. doi:10.1038/cr.2015.9
77. Monfared A, Ghaee A, Ebrahimi-Barough S. Preparation and characterisation of zein/polyphenol nanofibres for nerve tissue regeneration. *IET Nanobiotechnol*. 2019;13(6):571–577. doi:10.1049/iet-nbt.2018.5368

78. Abuarqoub D, Mahmoud NN, Zaza R, Abu-Dahab R, Khalil EA, Sabbah DA. The in vitro immunomodulatory effects of gold nanocomplex on THP-1-derived macrophages. *J Immunol Res*. 2022;2022:6031776. doi:10.1155/2022/6031776
79. Fang H, Zhu D, Yang Q, et al. Emerging zero-dimensional to four-dimensional biomaterials for bone regeneration. *J Nanobiotechnology*. 2022;20(1):26. doi:10.1186/s12951-021-01228-1
80. Colino CI, Lanao JM, Gutierrez-Millan C. Targeting of hepatic macrophages by therapeutic nanoparticles. *Front Immunol*. 2020;11:218. doi:10.3389/fimmu.2020.00218
81. Minnema LA, Giezen TJ, Gardarsdottir H, Egberts TCG, Leufkens HGM, Mantel-Teeuwisse AK. Post-marketing dosing changes in the label of biologicals. *Br J Clin Pharmacol*. 2019;85(4):715–721. doi:10.1111/bcp.13843
82. Haskins AH, Buglewicz DJ, Hirakawa H, Fujimori A, Aizawa Y, Kato TA. Palmitoyl ascorbic acid 2-glucoside has the potential to protect mammalian cells from high-LET carbon-ion radiation. *Sci Rep*. 2018;8(1):13822. doi:10.1038/s41598-018-31747-1
83. Chen X, Zou D, Chen X, Wu H, Xu D. Hesperetin inhibits foam cell formation and promotes cholesterol efflux in THP-1-derived macrophages by activating LXRalpha signal in an AMPK-dependent manner. *J Physiol Biochem*. 2021;77(3):405–417. doi:10.1007/s13105-020-00783-9
84. Kirca K, Kutluturkan S. Symptoms experience and quality of life in the patients with breast cancer receiving the taxane class of drugs. *Eur J Breast Health*. 2018;14(3):148–155. doi:10.5152/ejbh.2018.3785
85. Zeng L, Han Y, Chen Z, Jiang K, Golberg D, Weng Q. Biodegradable and peroxidase-mimetic boron oxynitride nanozyme for breast cancer therapy. *Adv Sci*. 2021;8(16):e2101184. doi:10.1002/advs.202101184
86. Yuan M, Zhang X, Wang J, Zhao Y. Recent progress of energy-storage-device-integrated sensing systems. *Nanomaterials*. 2023;13(4):645. doi:10.3390/nano13040645
87. Hosoyama K, Ahumada M, Goel K, Ruel M, Suuronen EJ, Alarcon EI. Electroconductive materials as biomimetic platforms for tissue regeneration. *Biotechnol Adv*. 2019;37(3):444–458. doi:10.1016/j.biotechadv.2019.02.011
88. Liu Z, Ji X, He D, Zhang R, Liu Q, Xin T. Nanoscale drug delivery systems in glioblastoma. *Nanoscale Res Lett*. 2022;17(1):27. doi:10.1186/s11671-022-03668-6
89. Liu M, Wang L, Lo Y, Shiu SC, Kinghorn AB, Tanner JA. Aptamer-enabled nanomaterials for therapeutics, drug targeting and imaging. *Cells*. 2022;11(1).
90. Zheng Y, Xue B, Wei B, et al. Core-shell oxygen-releasing fibers for annulus fibrosus repair in the intervertebral disc of rats. *Mater Today Bio*. 2023;18:100535. doi:10.1016/j.mtbio.2022.100535
91. Wang Z, Zhao Y, Shen M, Tomas H, Zhou B, Shi X. Antitumor efficacy of doxorubicin-loaded electrospun attapulgite-poly(lactic-co-glycolic acid) composite nanofibers. *J Funct Biomater*. 2022;13(2):55. doi:10.3390/jfb13020055
92. Alarcon Apablaza J, Lezcano MF, Godoy Sanchez K, Oporto GH, Dias FJ. Optimal morphometric characteristics of a tubular polymeric scaffold to promote peripheral nerve regeneration: a scoping review. *Polymers*. 2022;14(3):397. doi:10.3390/polym14030397
93. Zhao G, Hong L, Liu M, et al. Isolation and characterization of natural nanoparticles in naoluo xintong decoction and their brain protection research. *Molecules*. 2022;27(5).
94. Liang S, Zhang J, Liu Y, et al. Study on flavonoids and bioactivity features of pericarp of citrus reticulata "Chachi" at Different Harvest Periods. *Plants*. 2022;11(23). doi:10.3390/plants11233390
95. Qiao J, Lu G, Wu G, et al. Influence of different pretreatments and drying methods on the chemical compositions and bioactivities of Smilacis Glabrae Rhizoma. *Chin Med*. 2022;17(1):54. doi:10.1186/s13020-022-00614-7
96. He Q, Xiao H, Li J, et al. Fingerprint analysis and pharmacological evaluation of Ailanthus altissima. *Int J Mol Med*. 2018;41(5):3024–3032. doi:10.3892/ijmm.2018.3492
97. Sun J, Duan Z, Zhang Y, Cao S, Tang Z, Abozeid A. Metabolite profiles provide insights into underlying mechanism in Bupleurum (Apiaceae) in response to three levels of phosphorus fertilization. *Plants*. 2022;11(6).
98. Buyukgoz GG, Castro JN, Atalla AE, Pentangelo JG, Tripathi S, Dave RN. Impact of mixing on content uniformity of thin polymer films containing drug micro-doses. *Pharmaceutics*. 2021;13(6):812. doi:10.3390/pharmaceutics13060812
99. Shreffler JW, Pullan JE, Dailey KM, Mallik S, Brooks AE. Overcoming hurdles in nanoparticle clinical translation: the influence of experimental design and surface modification. *Int J Mol Sci*. 2019;20(23):6056. doi:10.3390/ijms20236056
100. Mehra R, Tjurmina OA, Ajijola OA, et al. Research opportunities in autonomic neural mechanisms of cardiopulmonary regulation: a report from the National Heart, Lung and Blood Institute and the National Institutes of Health Office of the Director Workshop. *JACC Basic Transl Sci*. 2022;7(3):265–293.
101. Petrov D, Burrell JC, Browne KD, et al. Neurorrhaphy in presence of polyethylene glycol enables immediate electrophysiological conduction in porcine model of facial nerve injury. *Front Surg*. 2022;9:811544. doi:10.3389/fsurg.2022.811544
102. Tao J, Wei X, Huang Y, et al. Sfrp1 protects against acute myocardial ischemia (AMI) injury in aged mice by inhibiting the Wnt/beta-catenin signaling pathway. *J Cardiothorac Surg*. 2021;16(1):12. doi:10.1186/s13019-020-01389-4
103. Farzin MA, Abdoos H, Saber R. AuNP-based biosensors for the diagnosis of pathogenic human coronaviruses: COVID-19 pandemic developments. *Anal Bioanal Chem*. 2022;414(24):7069–7084. doi:10.1007/s00216-022-04193-2
104. Dotan T, Jog A, Kadan-Jamal K, Avni A, Shacham-Diamand Y. In vivo plant bio-electrochemical sensor using redox cycling. *Biosensors*. 2023;13(2). doi:10.3390/bios13020219
105. Liao R, Lv P, Wang Q, Zheng J, Feng B, Yang B. Cyclodextrin-based biological stimuli-responsive carriers for smart and precision medicine. *Biomater Sci*. 2017;5(9):1736–1745. doi:10.1039/C7BM00443E
106. Cui J, Richardson JJ, Bjornmalm M, Faria M, Caruso F. Nanoengineered templated polymer particles: navigating the biological realm. *Acc Chem Res*. 2016;49(6):1139–1148. doi:10.1021/acs.accounts.6b00088
107. Sosnowski P, Sass P, Slonimska P, et al. Regenerative drug discovery using ear pinna punch wound model in mice. *Pharmaceuticals*. 2022;15(5):610. doi:10.3390/ph15050610
108. Evans CE, Iruela-Arispe ML, Zhao YY. Mechanisms of endothelial regeneration and vascular repair and their application to regenerative medicine. *Am J Pathol*. 2021;191(1):52–65. doi:10.1016/j.ajpath.2020.10.001
109. Zhao H, Liu L, Liu B, Wang Y, Li F, Yu H. An updated association between TNF-alpha −238G/A polymorphism and gastric cancer susceptibility in East Asians. *Biosci Rep*. 2018;38(6). doi:10.1042/BSR20181231

110. Guedon JM, Wu S, Zheng X, et al. Current gene therapy using viral vectors for chronic pain. *Mol Pain*. 2015;11:27. doi:10.1186/s12990-015-0018-1
111. Mai P, Hampl J, Baca M, et al. MatriGrid((R)) based biological morphologies: tools for 3D cell culturing. *Bioengineering*. 2022;9(5).
112. Wu W, Dong Y, Liu H, et al. 3D printed elastic hydrogel conduits with 7,8-dihydroxyflavone release for peripheral nerve repair. *Mater Today Bio*. 2023;20:100652. doi:10.1016/j.mtbio.2023.100652
113. Huang J, Liu F, Su H, et al. Advanced nanocomposite hydrogels for cartilage tissue engineering. *Gels*. 2022;8(2):138. doi:10.3390/gels8020138
114. Lu Y, Patton EE. Long-term non-invasive drug treatments in adult zebrafish that lead to melanoma drug resistance. *Dis Model Mech*. 2022;15(5). doi:10.1242/dmm.049401
115. Zou S, Wang Q, Zhang P, et al. Biomimetic nanosponges enable the detoxification of Vibrio vulnificus hemolysin. *Int J Mol Sci*. 2022;23(12):6821. doi:10.3390/ijms23126821
116. Gillman N, Lloyd D, Bindra R, Ruan R, Zheng M. Surgical applications of intracorporal tissue adhesive agents: current evidence and future development. *Expert Rev Med Devices*. 2020;17(5):443–460. doi:10.1080/17434440.2020.1743682
117. Presutti D, Agarwal T, Zarepour A, et al. Transition metal dichalcogenides (TMDC)-based nanozymes for biosensing and therapeutic applications. *Materials*. 2022;15(1):337. doi:10.3390/ma15010337
118. Jiraskova Zakostelska Z, Reiss Z, Tlaskalova-Hogenova H, Rob F. Paradoxical reactions to anti-TNFalpha and Anti-IL-17 treatment in psoriasis patients: are skin and/or gut microbiota involved? *Dermatol Ther*. 2023;13(4):911–933. doi:10.1007/s13555-023-00904-4
119. Lombardo F, Bombaci B, Costa S, et al. Gastroparesis in adolescent patient with type 1 diabetes: severe presentation of a rare pediatric complication. *J Clin Res Pediatr Endocrinol*. 2024;16(1):111–115. doi:10.4274/jcrpe.galenos.2022.2022-5-20
120. Joung D, Lavoie NS, Guo SZ, Park SH, Parr AM, McAlpine MC. 3D printed neural regeneration devices. *Adv Funct Mater*. 2020;30(1). doi:10.1002/adfm.201906237
121. Luo F, Sun TL, Nakajima T, et al. Free reprocessability of tough and self-healing hydrogels based on polyion complex. *ACS Macro Lett*. 2015;4(9):961–964. doi:10.1021/acsmacrolett.5b00501
122. Mathews DAP, Baird A, Lucky M. Innovation in urology: three dimensional printing and its clinical application. *Front Surg*. 2020;7:29. doi:10.3389/fsurg.2020.00029
123. Hu X, Wang J, Ju Y, et al. Combining metabolome and clinical indicators with machine learning provides some promising diagnostic markers to precisely detect smear-positive/negative pulmonary tuberculosis. *BMC Infect Dis*. 2022;22(1):707. doi:10.1186/s12879-022-07694-8
124. Kumar K, Kumar P, Deb D, Unguresan ML, Muresan V. Artificial intelligence and machine learning based intervention in medical infrastructure: a review and future trends. *Healthcare*. 2023;11(2).
125. Liu H, Zhang R, Liu Y, He C. Unveiling evolutionary path of nanogenerator technology: a novel method based on sentence-BERT. *Nanomaterials*. 2022;12(12).
126. Baik JM, Lee JP. Strategies for ultrahigh outputs generation in triboelectric energy harvesting technologies: from fundamentals to devices. *Sci Technol Adv Mater*. 2019;20(1):927–936. doi:10.1080/14686996.2019.1655663
127. Li Z, Tu Z, Wang H, Zhang L. Ultrasound-assisted extraction optimization of alpha-glucosidase inhibitors from Ceratophyllum demersum L. and identification of phytochemical profiling by HPLC-QTOF-MS/MS. *Molecules*. 2020;25(19):4507. doi:10.3390/molecules25194507
128. Bashir MA, Khan AU, Badshah H, Rodrigues-Filho E, Din ZU, Khan A. Synthesis, characterization, molecular docking evaluation, antidepressant, and anti-Alzheimer effects of dibenzylidene ketone derivatives. *Drug Dev Res*. 2019;80(5):595–605. doi:10.1002/ddr.21537